

ALEX TURNER



Extract from Robert Morden's map of Northumberland, 1695

Author

Alex Turner

Research Associate (Archaeology)

McCord Centre for Landscape

School of History, Classics and Archaeology

Newcastle University

Newcastle upon Tyne

NE1 7RU

# Table of Contents

Table of Contents .....	1
Table of Figures .....	2
Introduction.....	4
Location .....	4
Survey Conditions.....	4
Survey location – satellite and aerial imagery.....	5
Topography and Geology .....	6
Topography – Lidar .....	6
Geology.....	7
Survey Methodology .....	9
Methods - Survey Grids and Markers.....	9
Methods – Ground-penetrating Radar (GPR).....	9
Methods - Fluxgate gradiometer survey .....	10
Methods – Electrical resistance survey .....	11
Data processing and presentation.....	12
Reference to Historic Ordnance Survey .....	12
Identified Features .....	12
Survey Results and Interpretation.....	17
GPR plot of results .....	17
Processing flow.....	20
GPR - Interpretation .....	21
GPR – Interpretation overlays .....	22
Gradiometer – plots of results .....	26
Gradiometer Overlays .....	29
Gradiometer – Interpretation .....	32
Resistivity Results – process summary .....	32
Resistivity – plot of results.....	33
Resistivity – Interpretation Overlays .....	34
Resistivity – Interpretation .....	35
Summary.....	36
Sources and References .....	36

## Table of Figures

Figure 1 - Location of the Heddon-on-the-Wall survey area .....	4
Figure 2 - Survey locations superimposed on Google Earth image 12th July 2021 .....	5
Figure 3 - Survey locations superimposed on Google Earth image 2002 .....	5
Figure 4 - Survey locations superimposed on Google Earth aerial photographs 1945.....	5
Figure 5 - Survey locations superimposed on DTM hillshade of one metre resolution lidar data .....	6
Figure 6 - Survey locations superimposed on DSM hillshade of one metre resolution lidar data .....	6
Figure 7 - Location of the topographic profiles .....	7
Figure 8 - Topographic profiles running north-south through the survey areas .....	7
Figure 9 - Survey locations superimposed on 1:10,000 British Geological Survey map of bedrock.....	8
Figure 10 - Survey locations superimposed on 1:10,000 British Geological Survey map of Superficial geology.....	8
Figure 11 - Survey locations superimposed on 1:10,000 British Geological Survey map of Artificial geology .....	8
Figure 12 - Survey locations superimposed on British Geological Survey 1:10,000 Soil parent map.....	9
Figure 13 - Location of the GPR survey for 2018 .....	9
Figure 14 - Location of the gradiometer survey 2018 .....	10
Figure 15 - Location of the GPR survey 2019.....	10
Figure 16 - Location of the electrical resistance survey March 2019 .....	11
Figure 17 - Location of the electrical resistance survey September 2019.....	11
Figure 18 - Location of western survey areas superimposed on County Series 1:2500 map published in 1859.....	12
Figure 19 - Location of western survey areas superimposed on County Series 1:2500 map published in 1897.....	12
Figure 20 - Location of western survey areas superimposed on County Series 1:2500 map published in 1920.....	13
Figure 21 - Location of western survey areas superimposed on National Grid 1:2500 map published in 1963 .....	<b>Error!</b>
<b>Bookmark not defined.</b>	
Figure 22 - Location of eastern survey areas superimposed on National Grid 1:2500 map published in 1859 .....	14
Figure 23 - Location of eastern survey areas superimposed on National Grid 1:2500 map published in 1879 .....	14
Figure 24 - Location of eastern survey areas superimposed on National Grid 1:2500 map published in 1920 .....	15
Figure 25 - Location of eastern survey areas superimposed on National Grid 1:2500 map published in 1964 .....	15
Figure 26 - Location of coal pits on the County Series 1:2500 First Edition for 1859 superimposed on the 1945 aerial photograph derived from Google Earth.....	16
Figure 27 - Location of coal pits on the County Series 1:2500 First Edition for 1859 superimposed on the 2021 satellite image derived from Google Earth.....	16
Figure 28 - Plot of GPR data at c20cm depth.....	17
Figure 29 - Plot of GPR data at c40cm depth.....	17
Figure 30 - Plot of GPR data at c60cm depth.....	18
Figure 31 - Plot of GPR data at c80cm depth.....	18
Figure 32 - Plot of GPR data at c100cm depth.....	19
Figure 33 - Plot of GPR data at c120cm depth.....	19
Figure 34 - Plot of GPR data at c140cm depth.....	20
Figure 35 - Interpretation of the GPR survey at c20cm depth.....	22
Figure 36 - Interpretation of the GPR survey at c40cm depth.....	22
Figure 37 - Interpretation of the GPR survey at c60cm depth.....	23
Figure 38 - Interpretation of the GPR survey at c80cm depth.....	23
Figure 39 - Interpretation of the GPR survey at c100cm depth.....	24
Figure 40 - Interpretation of the GPR survey at c120cm depth.....	24
Figure 41 - Interpretation of the GPR survey at c140cm depth.....	25
Figure 42 - Plot of gradiometer survey results - Areas A and B 2018 .....	26
Figure 43 - Plot of gradiometer survey results - Area C 2018.....	27
Figure 44 - Plot of gradiometer survey results - Areas 1 and 2 2019 .....	27
Figure 45 - Plot of gradiometer survey results - Area 3 2019.....	28
Figure 46 - Interpretation of gradiometer survey results - Area A 2018 .....	29
Figure 47 - Interpretation of gradiometer survey results - Area B 2018 .....	29
Figure 48 - Interpretation of gradiometer survey results - Area c 2018.....	30

Figure 49 - Interpretation of gradiometer survey results - Area 1 2019 .....	30
Figure 50 - Interpretation of gradiometer survey results - Area 2 2019 .....	31
Figure 51 - Interpretation of gradiometer survey results - Area 3 2019 .....	31
Figure 53 - Plot of the resistivity survey results - Area 2 September 2019.....	33
Figure 54 - Plot of the resistivity survey results - Area 1 September 2019.....	33
Figure 55 - Interpretation of the resistivity survey results - March 2019.....	34
Figure 56 - Interpretation of the resistivity survey results - Area 2 September 2019 .....	34
Figure 57 - Interpretation of the resistivity survey results - Area 1 September 2019 .....	35



## Introduction

As part of the Hadrian's Wall Community Archaeology Project, three sessions of geophysical survey were undertaken in 2018 and 2019. The first, in 2018, was part of the pilot stage for the project and concentrated on the western end of the study area. The work in 2019 expanded on the earlier surveys both in terms of area and methodologies employed. A combination of ground-penetrating radar (GPR), gradiometer and resistivity surveys were employed alongside a topographic assessment of the vallum and were carried out by volunteers under the supervision of members of the WallCAP team.

## Location

The site is located between the villages of Heddon-on-the-Wall to the west and Throckley to the east. It is approximately 11 kilometres west of Newcastle city centre. (Figure 1). The site is centred on Ordnance Survey grid reference NZ 14400 66800.

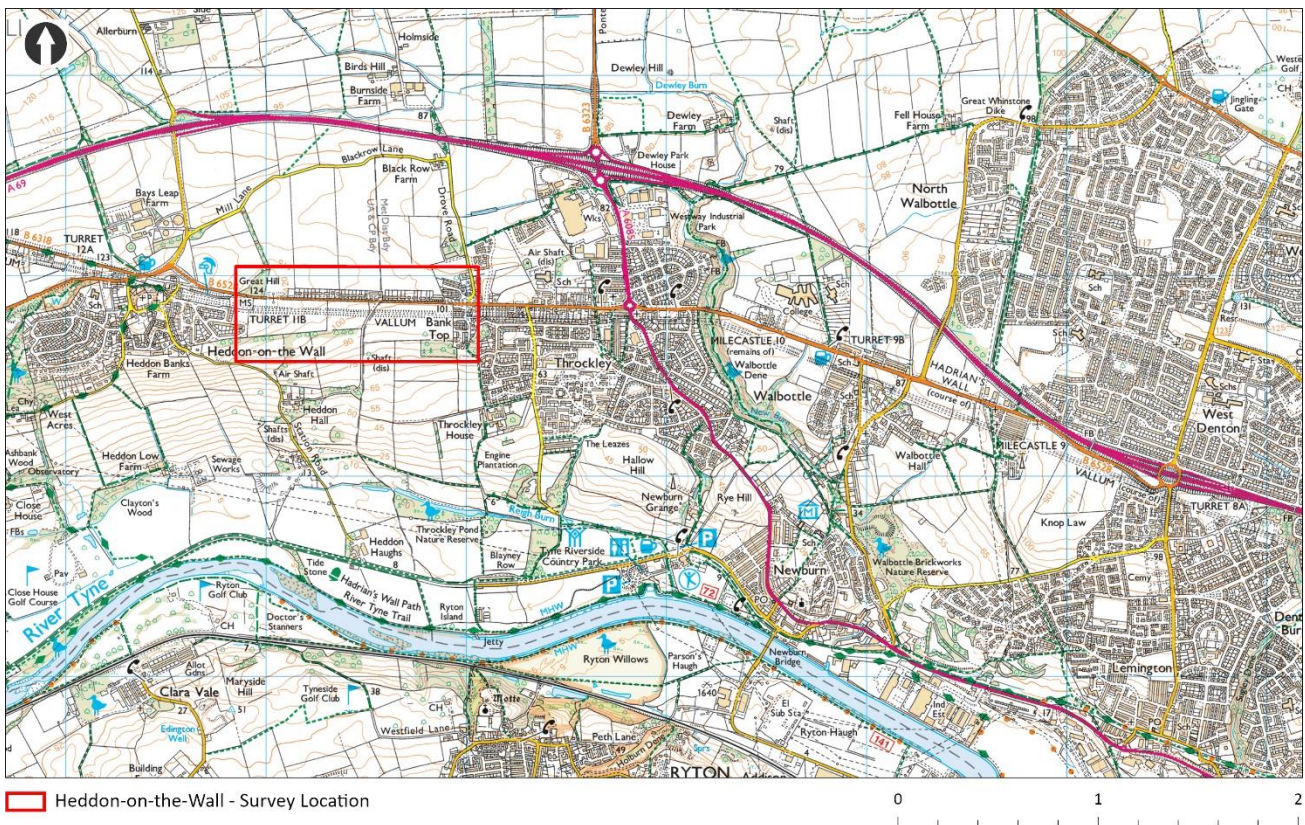


Figure 1 - Location of the Heddon-on-the-Wall survey area

## Survey Conditions

The 2018 survey area was laid to pasture and was bounded on its northern edge by a hedgeline that ran along the line of the B6528 Hexham Road. The 2019 survey was undertaken in two stages. The session in March at the western end of the survey area was, like the 2018 survey, laid to pasture. The session in September at the eastern end of the survey area was covered with stubble from recent harvesting. Both sets of ground conditions were ideal for gradiometer and resistivity survey but the GPR survey was only successful in 2018 and only reached a maximum depth of 1.4 metres due to the attenuation of signal caused by ground moisture. A further GPR survey attempt in March 2019 was unsuccessful due to a combination of ground conditions and technical problems with the survey equipment. Although the survey team was largely inexperienced and progress was slower as a result, the rate of progress was sufficient enough to obtain a number of high quality sets of data from across the survey area.



## Survey location – satellite and aerial imagery



Figure 2 - Survey locations superimposed on Google Earth image - 12th July 2021



Figure 3 - Survey locations superimposed on Google Earth image - 2002



Figure 4 - Survey locations superimposed on Google Earth aerial photographs - 1945



The survey areas were superimposed on a combination of satellite and aerial imagery derived from Google Earth. Comparisons of the surveys on the 2021 and 2002 images show that the line of the vallum was more easily identified at the western end of the survey area, where today it is a much more significant earthwork, than at the eastern end. On the 2021 image the earthwork is not detectable at the eastern end and is seen as a faint band on the 2002 image. Conversely the aerial image from 1945 shows the same earthwork as a clearly visible band at the eastern end and less clearly at the western end. The 1945 photographs are vertical rather than oblique and this could be responsible for the lack of visibility. This monochrome image does, however, clearly show the former divisions with the present field. One such boundary was observed running north-south through the western side of the 2019 area 2 gradiometer survey. Despite this observation, any trace of the boundary was not detected in the survey data.

## Topography and Geology

### Topography – Lidar

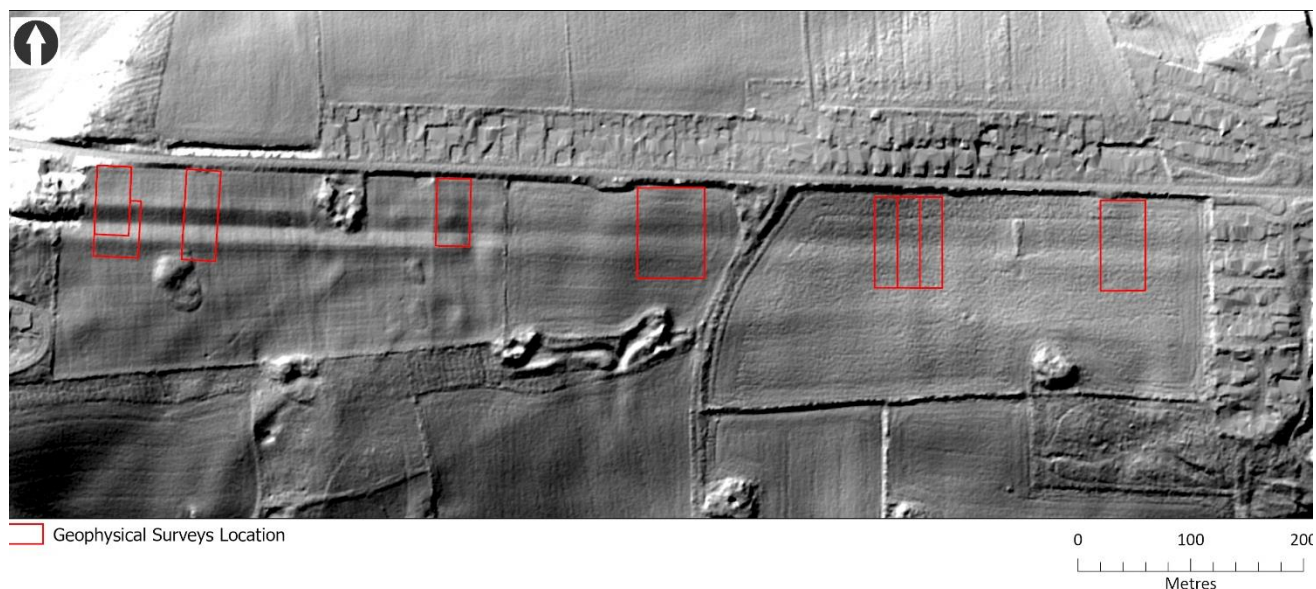


Figure 5 - Survey locations superimposed on DTM hillshade - one metre resolution lidar data



Figure 6 - Survey locations superimposed on DSM hillshade - one metre resolution lidar data

Examination of the Environment Agency lidar data Digital Terrain Model (Figure 5) and Digital Surface Model (Figures 6) show an 11.5m north-south slope across the western end of the survey (Figure 7, Transect 1).

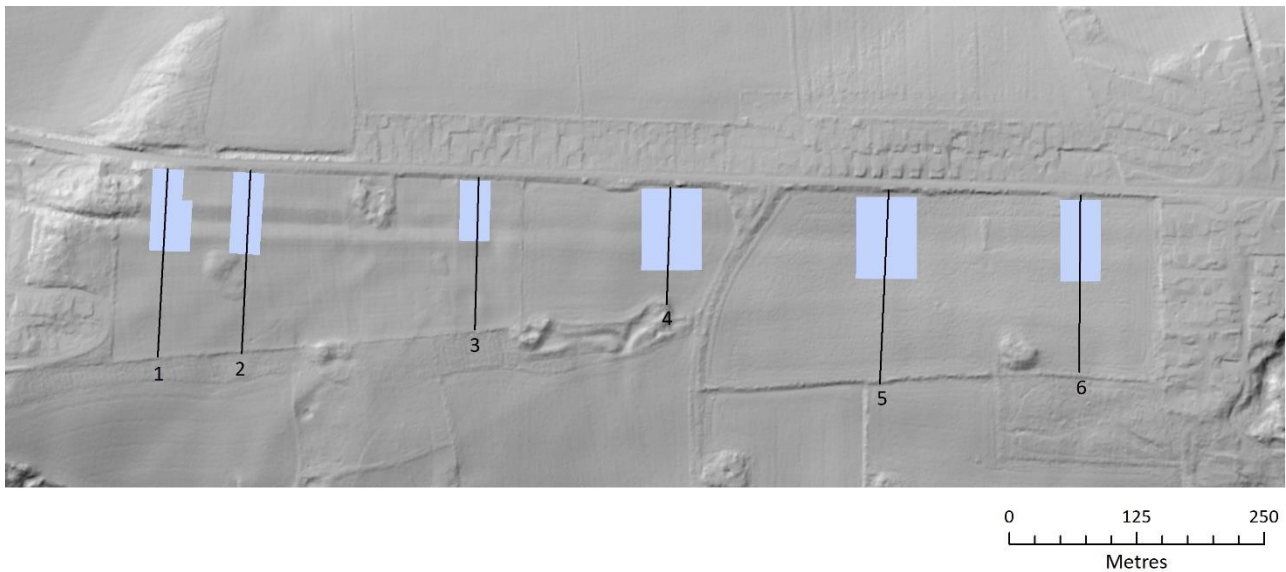


Figure 7 - Location of the topographic profiles

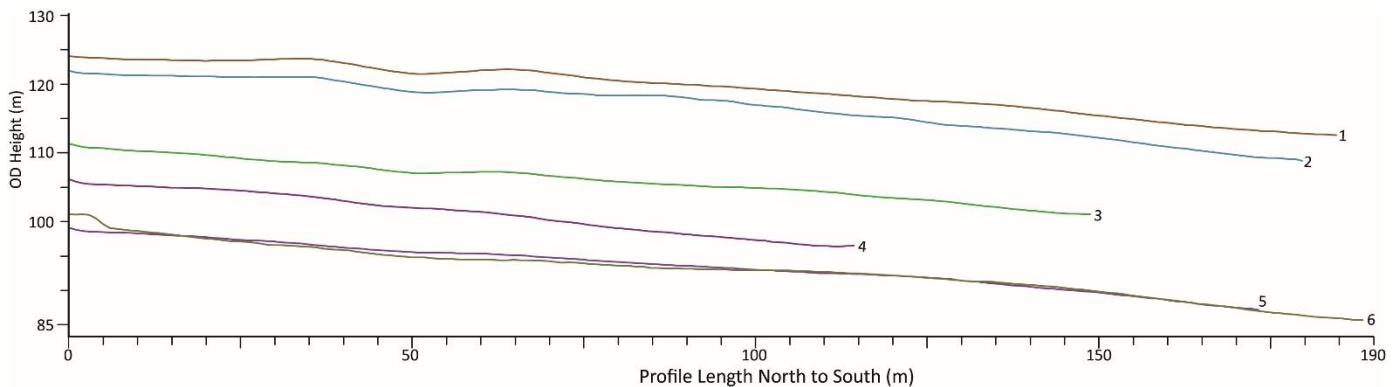


Figure 8 - Topographic profiles running north-south through the survey areas

At the eastern end of the survey the north-south slope is even greater at 11.93m (Figure 7, Transect 6). In the smaller field at the centre of the survey the north-south slope was 9.69m (Figure 7, Transect 4). The maximum difference in height in an east-west direction is 24.97m at the northern edge of the survey area and 25.38m at the southern edge of the survey. The most noticeable change in topography, within individual survey areas, relates to the presence of the vallum and shows a significantly greater earthwork at the western edge of the survey (Figure 8, Transect 1) than at the eastern edge (Figure 8, Transect 6). The transition occurs from west-east and mirrors the change from pasture to arable. The results of the near surface geophysical surveys confirm that the response towards the eastern end the survey area is lower than that at the western end.

## Geology

The bedrock geology for western half of the survey is Pennine Lower and Coal Measures with mudstone, siltstone and sandstone. The eastern bedrock geology is Pennine Middle Coal Measures, also with mudstone, siltstone and sandstone. The existence of a number of coal workings shown on the late 19<sup>th</sup> century maps is a testament to this. The superficial geology is classified as Till (Diamicton) and is a mixture of clay, sand, gravel and boulders that vary widely in size and shape. This variation in superficial geology may account for some of the poor responses from the ground-penetrating radar (GPR). There are also a number of areas of made or infilled ground that are detailed in the British Geological Survey Artificial layer and although none of these



appear to directly correspond with any of the survey areas, it is highly likely that some early extraction sites have remained unmapped. The soil type is described as loam-clay with bands of clay-loam and loam.



Figure 9 - Survey locations superimposed on 1:10,000 British Geological Survey map of Bedrock geology.



Figure 10 - Survey locations superimposed on 1:10,000 British Geological Survey map of Superficial geology.

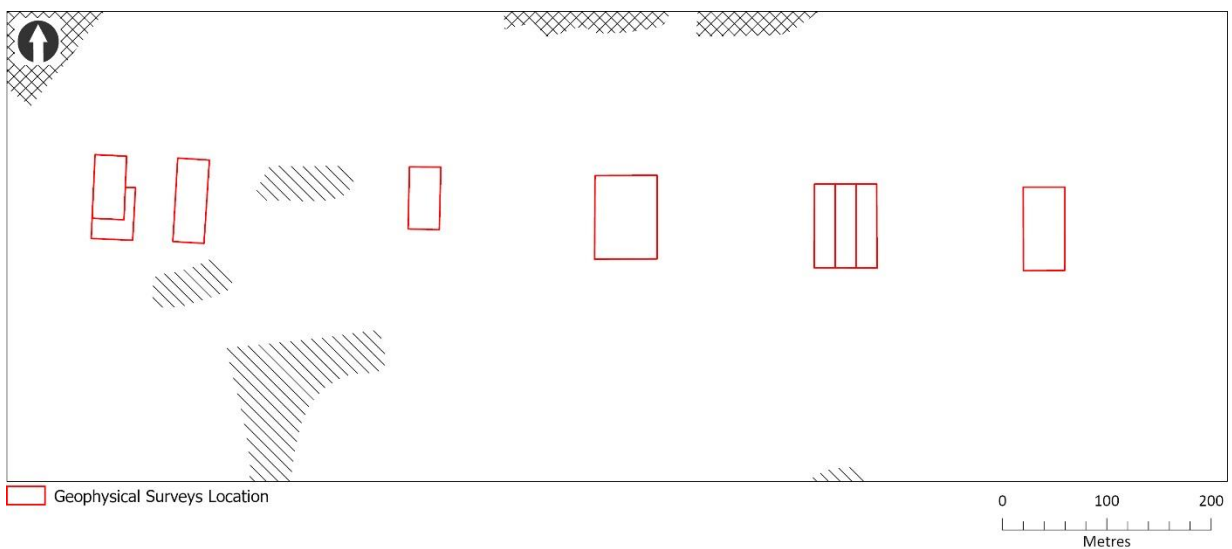


Figure 11 - Survey locations superimposed on 1:10,000 British Geological Survey map of Artificial geology

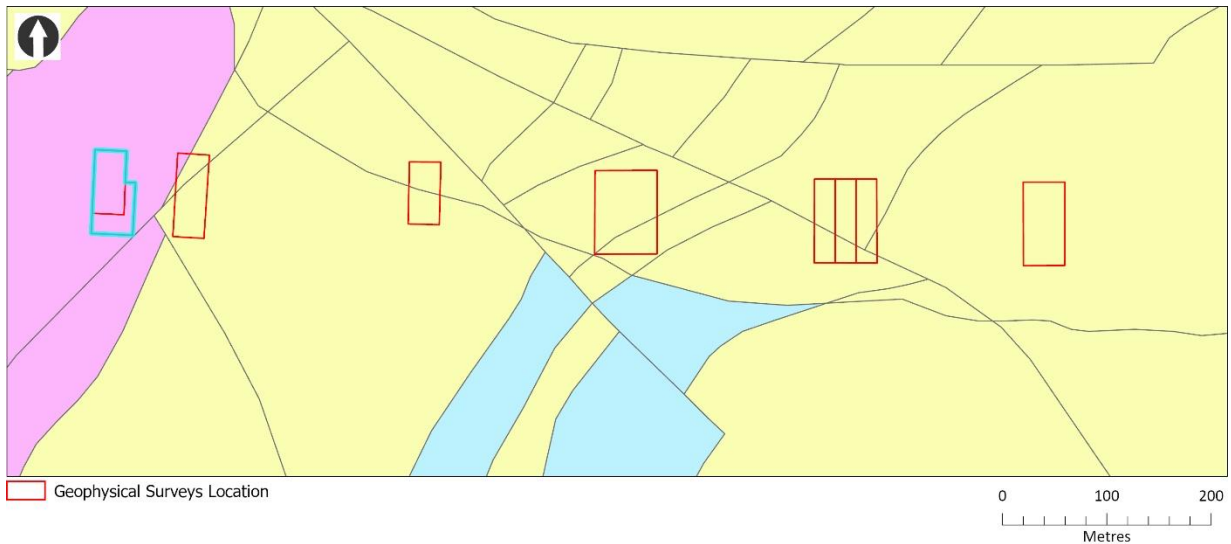


Figure 12 - Survey locations superimposed on 1:10,000 Soil British Geological Survey parent map

## Survey Methodology

### Methods - Survey Grids and Markers

For the 2018 gradiometer survey and GPR survey, the grids were laid out as a series of 30m x 30m squares using a Leica GNSS differential survey grade GPS connected to the Leica RTK Smartnet network. This grid size was also used for the resistivity survey in March 2019. However, after a review of the logistical problems of completing 30m x 0.5m x 0.5m resistance survey grids within the time allocated, it was decided to switch to using a smaller 20m x 20m survey unit, as this was more flexible within the restricted working day. Temporary grid pegs were used to mark out the grid and the lack of livestock in the fields meant these could be left in place overnight. The survey grid coordinates were derived from Mastermap digital data and stored as a feature class within the survey ArcGIS geodatabase. Survey areas were given letters in 2018 and numbers in 2019 to avoid confusion. Some areas were surveyed in both years. Grids were numbered north to south within each area. Where possible, the gradiometer grid layout was chosen to avoid any close proximity to the ferrous interference within the field. The areas covered by resistivity survey and GPR were unaffected by ferrous intrusions.

### Methods – Ground-penetrating Radar (GPR)

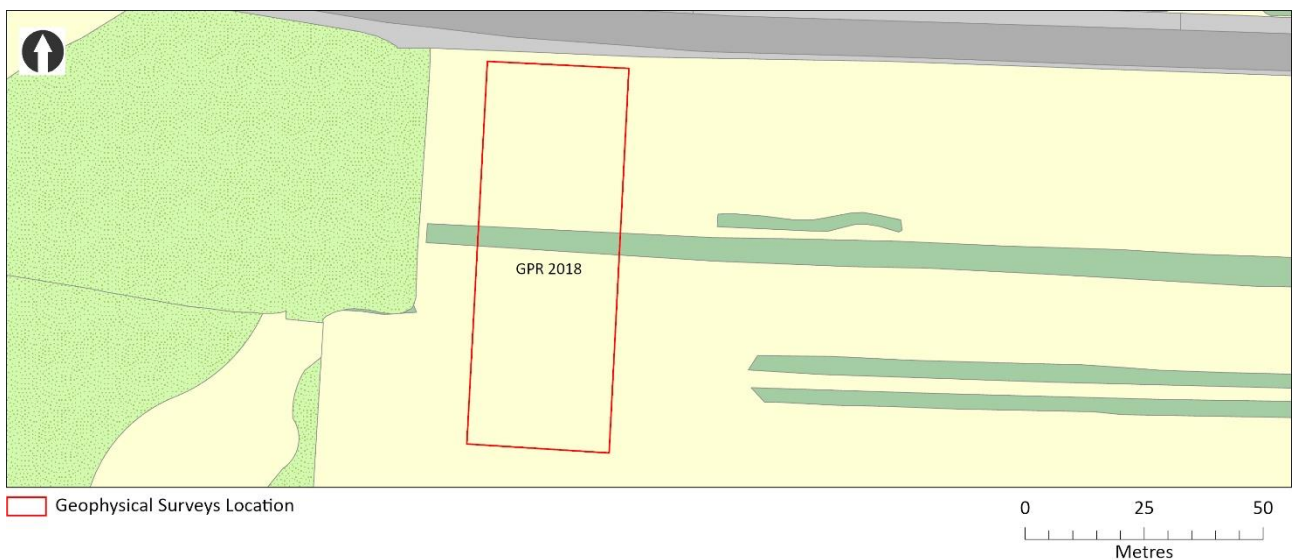


Figure 13 - Location of the GPR survey for 2018

The GPR survey was carried out using an UTSI Groundvue 3 single channel radar controller with a 400mhz antenna. Based on previous experience of similar survey conditions, this was considered to be the correct frequency for the depth of survey required and enabled the collection of data with a detectable vertical resolution of c.40 mm. 120 x 30 metre transect lines were laid out in two adjacent blocks with an east-west separation of 0.5m metre and a north-south trace interval of 0.05 metres. Each trace collected 256 vertical samples and wa walked in the same north-south direction. Although more time consuming, this was done to improve the consistency between lines when using inexperienced operators. Closer spacing of the transects was considered but within the time constraints of the survey it was deemed important to maximise coverage at the expense of a higher survey resolution. The GPR data was processed using ReflexW 9.5.6 (Sandmeier 2021) processing software to produce both 2D vertical profiles and 3D XY time slices. All the resultant plots from the data were transferred to an ArcGIS Pro project where they were georeferenced to the real-world using data collected with a Leica GNSS survey grade GPS. This also allowed a comparison with a range of other data sets collected as part of the construction of the GIS.

### Methods - Fluxgate gradiometer survey

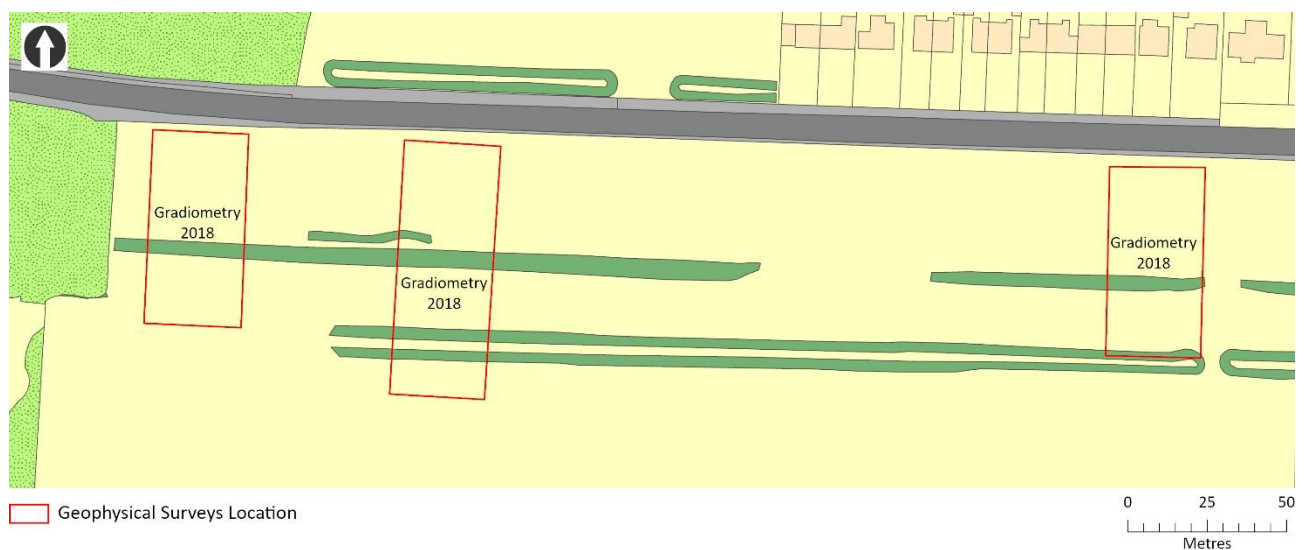


Figure 14 - Location of the gradiometer survey 2018

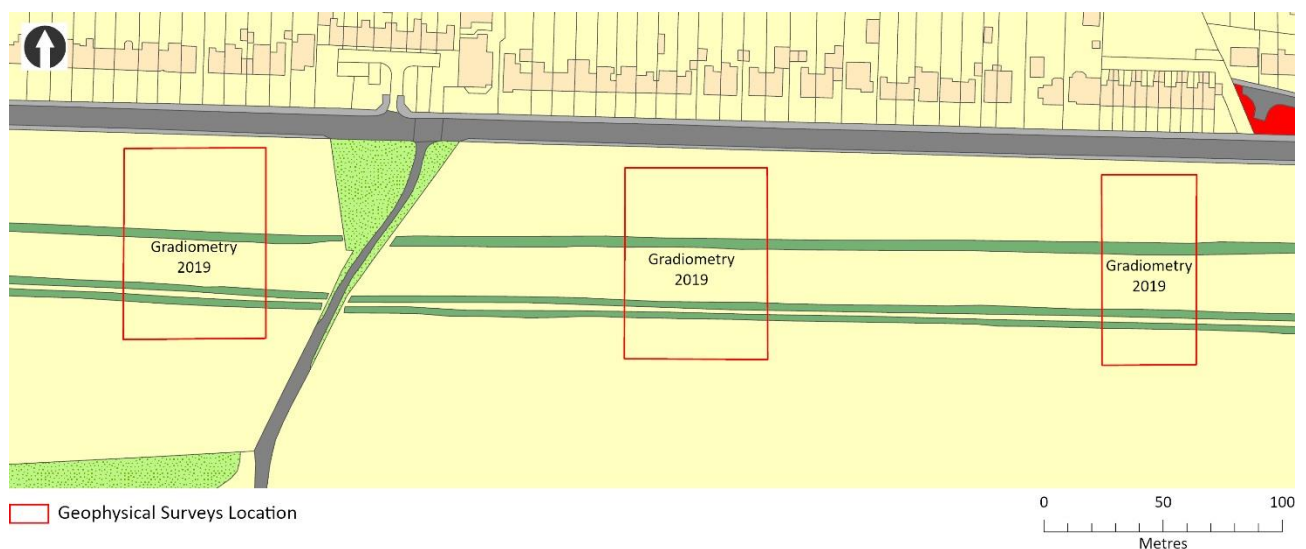


Figure 15 - Location of the GPR survey 2019

The survey was carried out using a Bartington Grad 601/2 fluxgate gradiometer with two vertical sensors spaced one metre apart. Following an initial scan of the survey site, a magnetically sterile area was identified



for the creation of the survey control point. This was used to calibrate the gradiometer before each day of survey and after any significant stoppages. In accordance with accepted practice (Schmidt et al 2016, 12) data was collected along a series of zig-zag traverses spaced one meter apart with sample readings being taken every 25 centimetres. This gave an effective resolution of 3600 readings for each 30m x 30m survey grid and 1600 readings for each 20m x 20m square.

### Methods – Electrical resistance survey

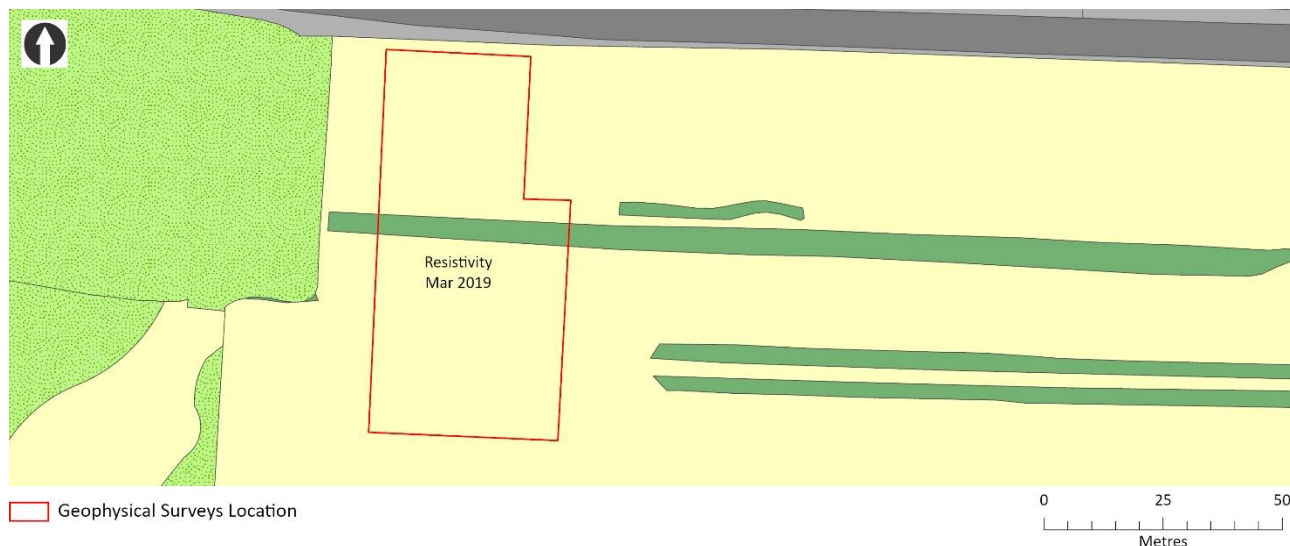


Figure 16 - Location of the electrical resistance survey March 2019

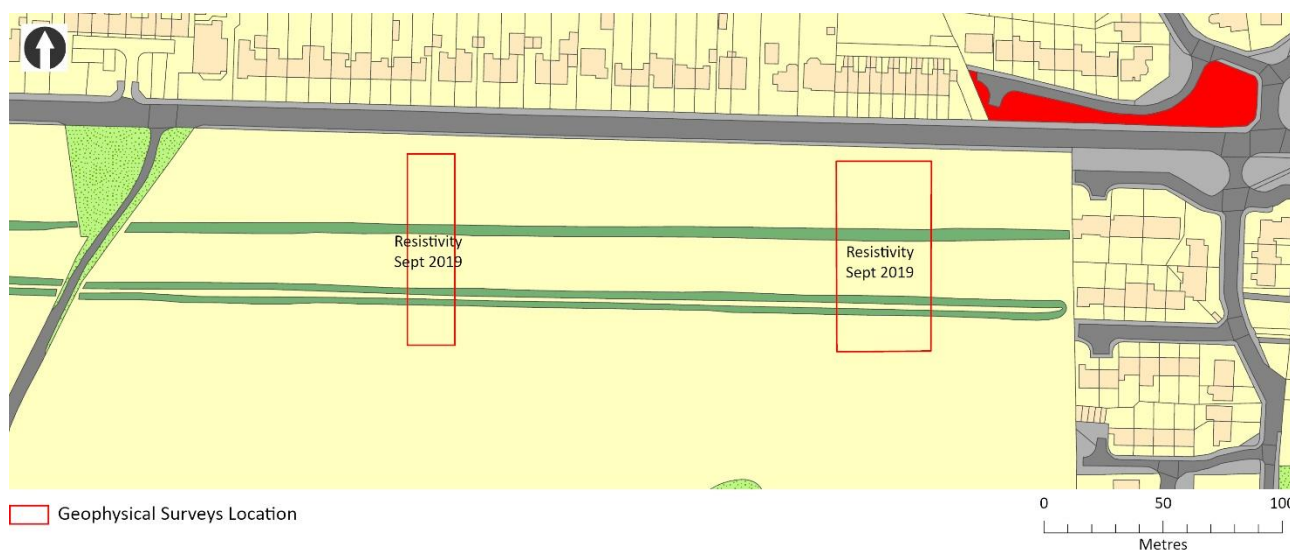


Figure 17 - Location of the electrical resistance survey September 2019

Electrical resistance survey was carried out using a Geoscan RM15D Advanced equipped with a MPX15 multiplexer collecting data in parallel twin configuration. The data was collected using a 0.5 metre traverse separation and a sample collection interval of 0.5 metre to provide a resolution of survey four times greater than a standard 1 metre x 1 metre survey. This gave a resolution for each 30mx30m survey grid of 3600 readings and 1600 readings for each 20m x 20m survey grid. The enhanced survey resolution significantly impacted survey speed but the enhanced detail provided during the interpretation of the results clearly justified this decision.

## Data processing and presentation

The data from both the resistivity and gradiometer surveys were processed using Geoplot 4.0. The resulting plots were exported as raster images to ArcGIS 7.1 where they were scaled and georeferenced using the latest vectored Mastermap data. This enabled comparison with a combination of modern and historic Ordnance Survey mapping data, Environment Agency Lidar data and aerial photographs downloaded from Digimap. The integration of digital output from the geophysical survey with the Digital Terrain Model (DTM) obtained from the Environment Agency Lidar data also enabled detailed topographic examination of the survey terrain. Digital overlays were created for features identified within the survey output and formed the basis of the final interpretation of the data.

## Reference to Historic Ordnance Survey

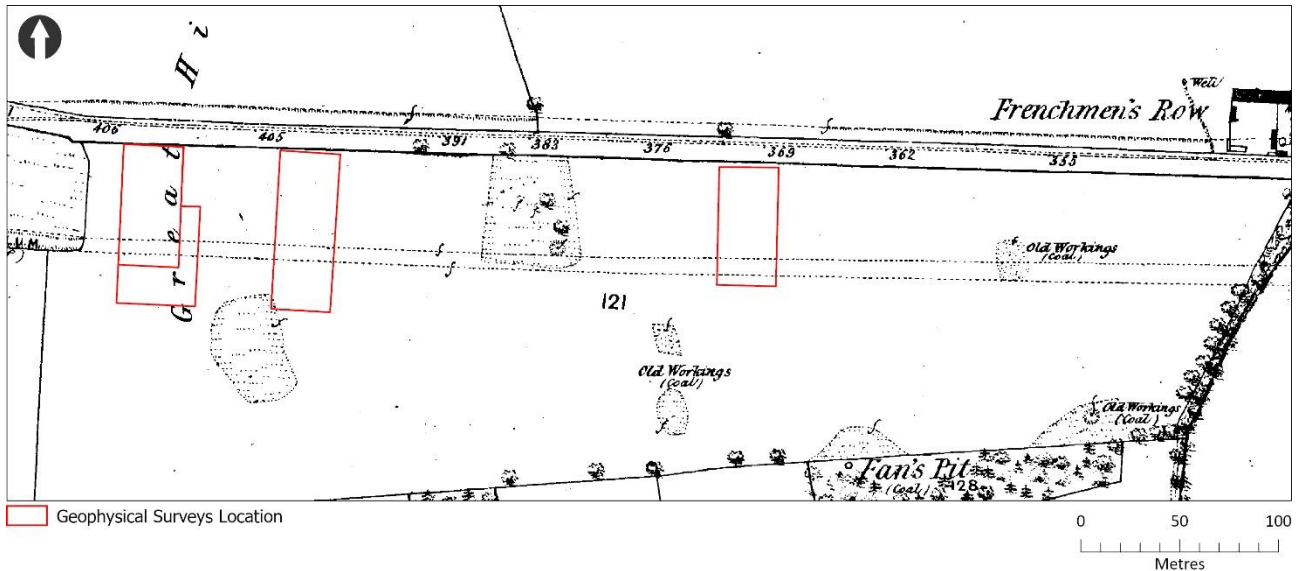


Figure 18 - Location of western survey areas superimposed on County Series 1:2500 map published in 1859

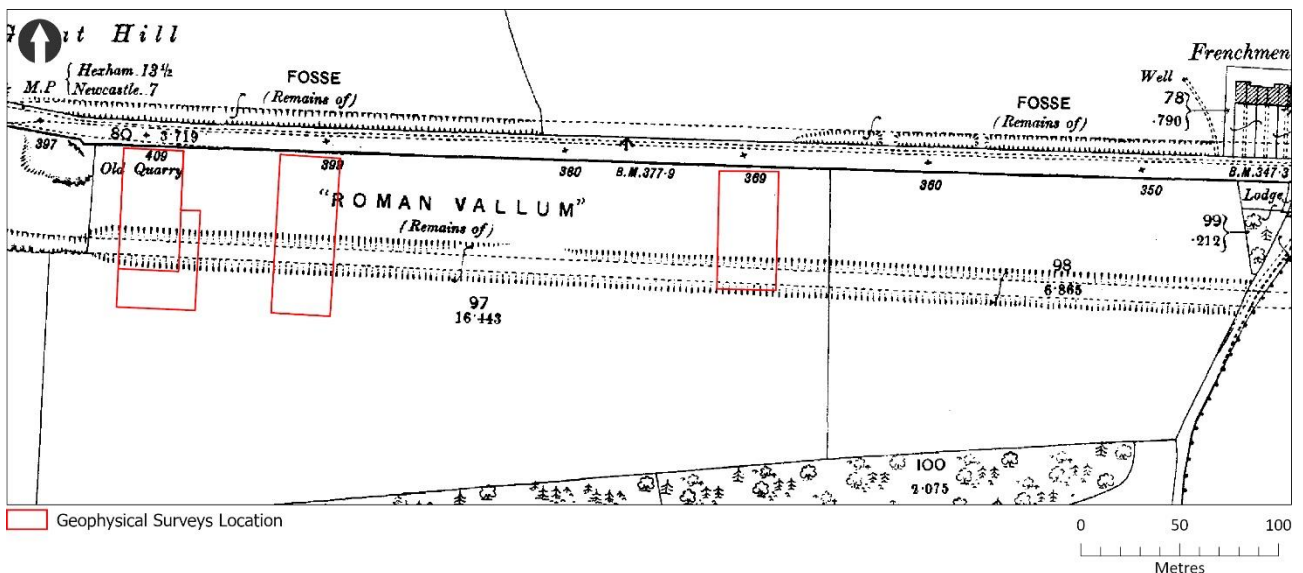


Figure 19 - Location of western survey areas superimposed on County Series 1:2500 map published in 1897

## Identified Features

An examination of the Ordnance Survey County Series 1:2500 map, published in 1859, showed a series of features described in some cases as “Old Workings (coal)” and in other cases as just pictorial representations of rough ground with pits (Figure 18). One area in particular coincides with a waste dump that is known to

contain late 19th century rubbish. It is currently covered by a stand of trees (Figure 27). The stand of trees and the current level of ground disturbance must date post 1945 as the aerial photograph for that year shows neither an area of disturbance nor of trees (Figure 26). The features on the 1859 map are not included on the publication of the 1897 County Series 1:2500 First Revision and are absent from all further 1:2500 editions (Figures 19-21). The coal workings appear to be largely limited to the western end of the survey area but coal

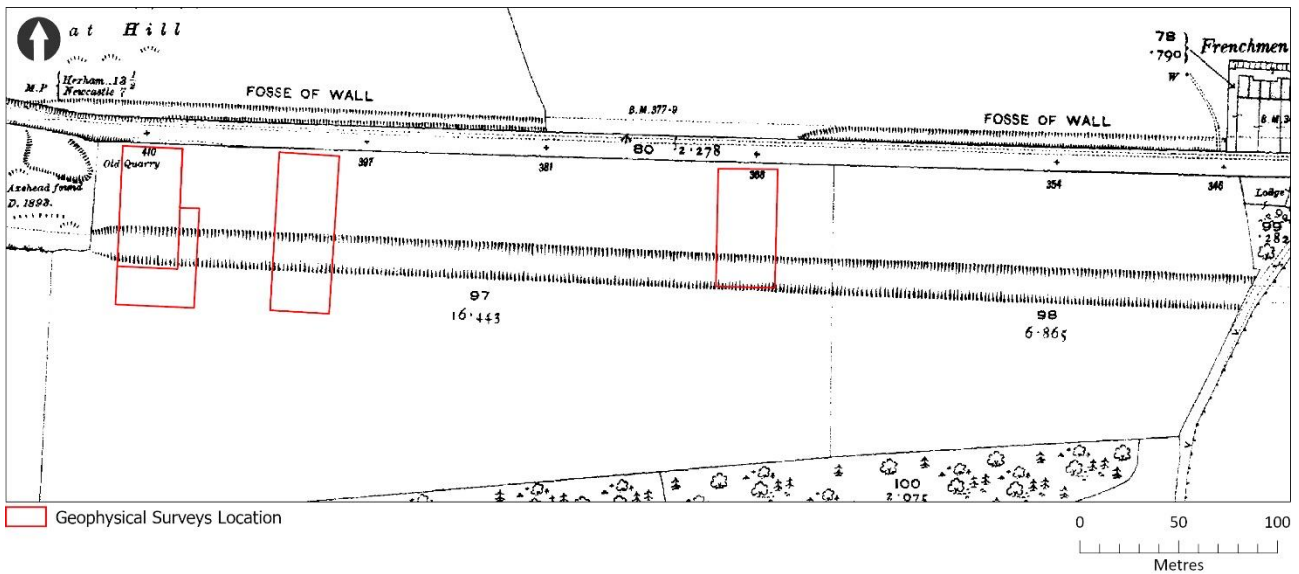


Figure 20 - Location of western survey areas superimposed on County Series 1:2500 map published in 1920

pits rather coal workings are shown on the 1859 map for the eastern end (Figure 22) but these are at least 50m south of the survey areas. These features persist on the subsequent editions of both the County Series and National Grid 1:2500 maps and are delineated by a boundary enclosing a stand of trees. Other features that are shown on the County Series editions of the Ordnance Survey 1:2500 maps are the site of Milecastle 11 which is located in the north-east corner of 2019 survey area 3. This feature is not recorded in this position on the 1:2500 National Grid series and presumably coincides with the formation of the opinion that

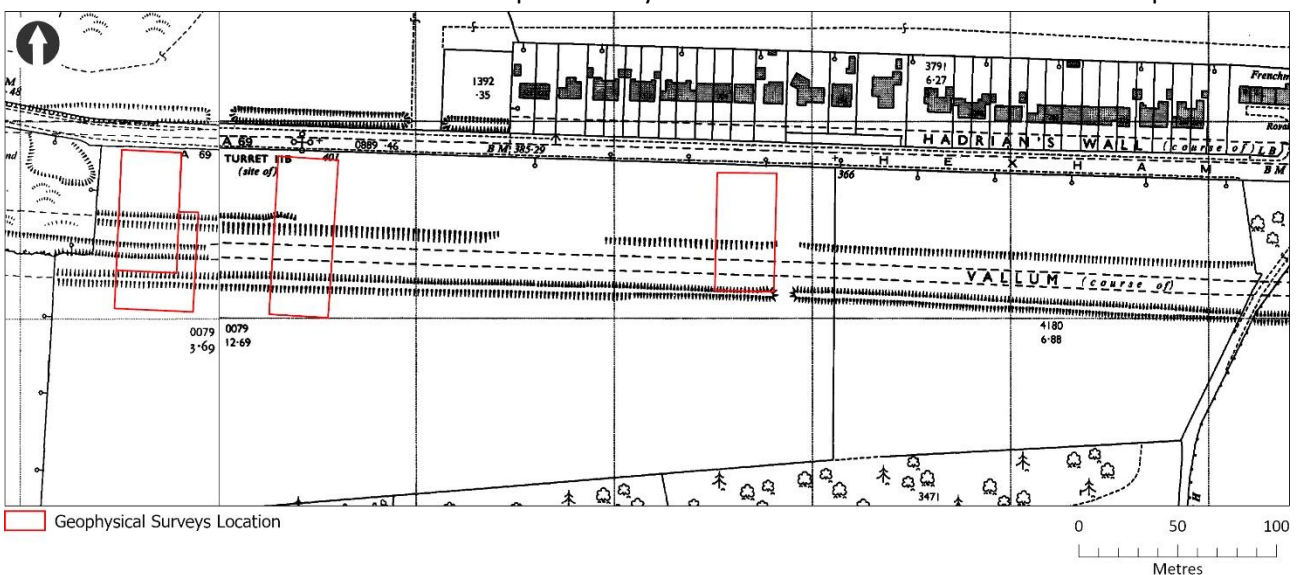


Figure 21 - Location of western survey areas superimposed on National Grid 1:2500 map published in 1963

Milecastle 11 is located under the Throckley and District Bank Top Club (Breeze 2006, 165), although no structural evidence has been discovered for this site in this position either. Turrets 11a and 11b are purported to be located on the northern edge of the west end of the survey area. There is currently no evidence for the location of Turret 11a and the 2019 gradiometer survey, although in close proximity to its measured location, failed to find any confirmatory evidence for its existence. The proposed site for Turret 11b (Great Hill), based



on finds of pottery and occupation layers in 1928 (Breeze 2006, 165), lies in close proximity to the northern edge of the 2018 gradiometer survey area B but as with Turret 11a no evidence of a structure was found during the survey.

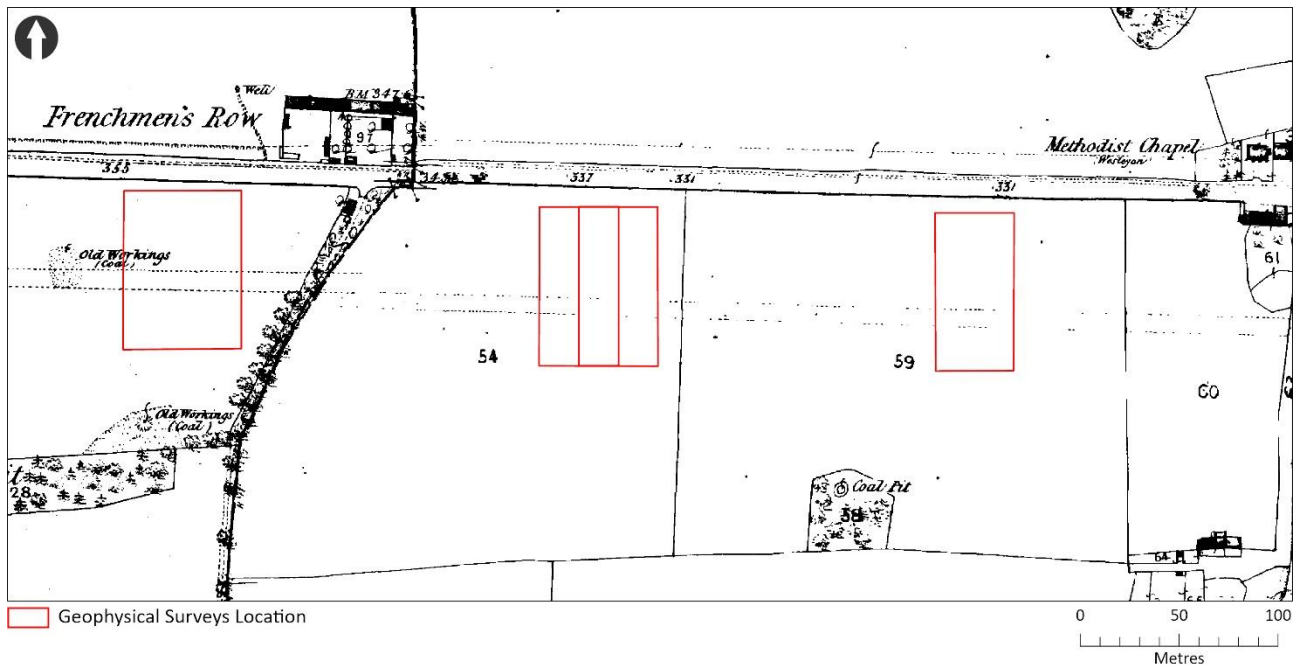


Figure 22 - Location of eastern survey areas superimposed on National Grid 1:2500 map published in 1859

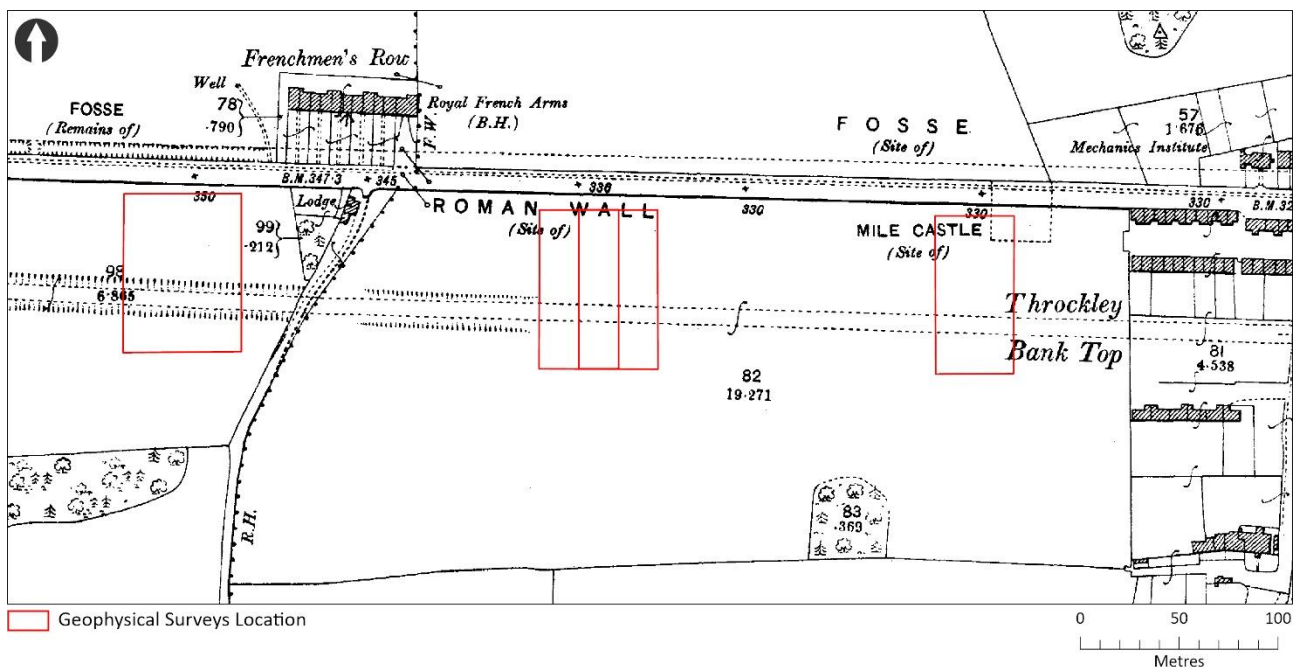


Figure 23 - Location of eastern survey areas superimposed on National Grid 1:2500 map published in 1879

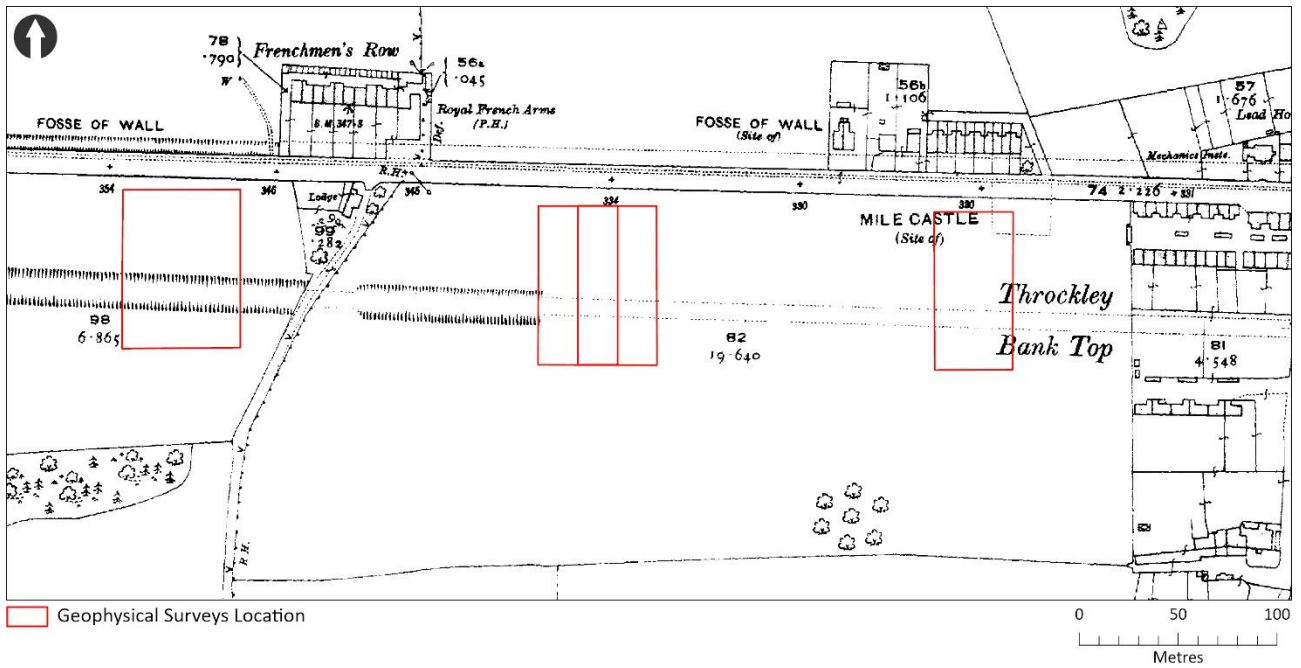


Figure 24 - Location of eastern survey areas superimposed on National Grid 1:2500 map published in 1920

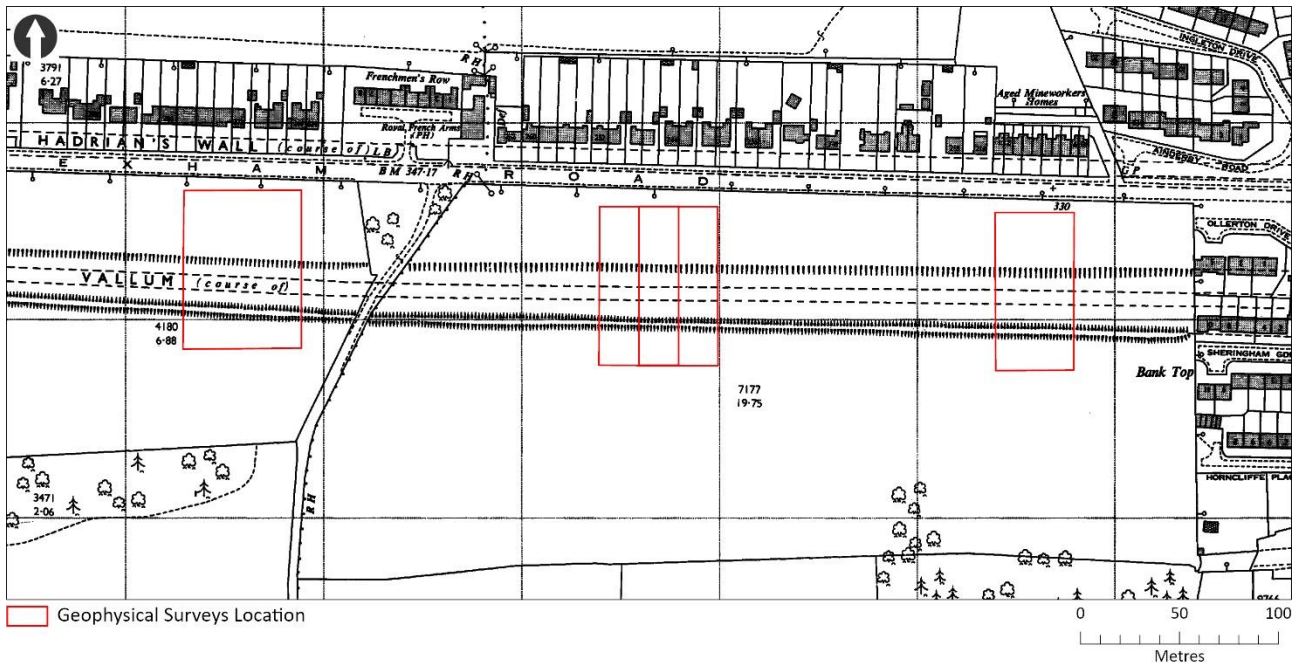


Figure 25 - Location of eastern survey areas superimposed on National Grid 1:2500 map published in 1964

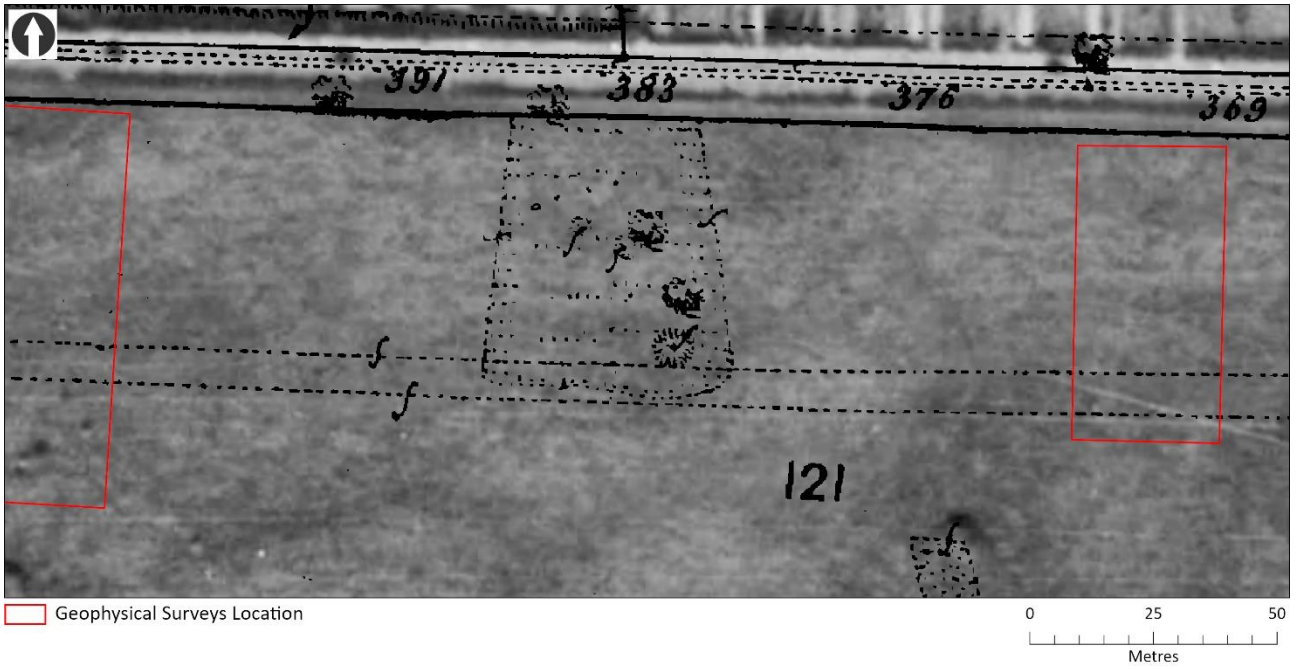


Figure 26 - Location of coal pits on the County Series 1:2500 First Edition for 1859 superimposed on the 1945 aerial photograph derived from Google Earth



Figure 27 - Location of coal pits on the County Series 1:2500 First Edition for 1859 superimposed on the 2021 satellite image derived from Google Earth



# Survey Results and Interpretation

## GPR plot of results



Figure 28 - Plot of GPR data at c20cm depth

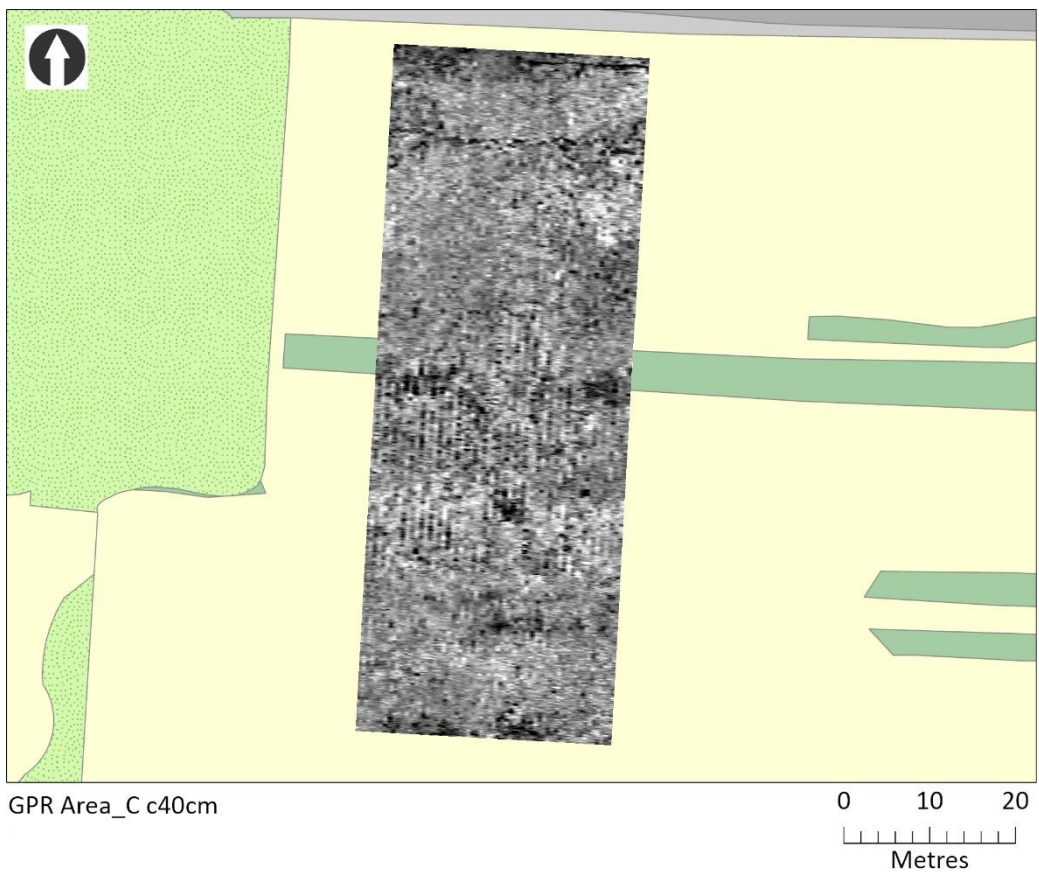


Figure 29 - Plot of GPR data at c40cm depth

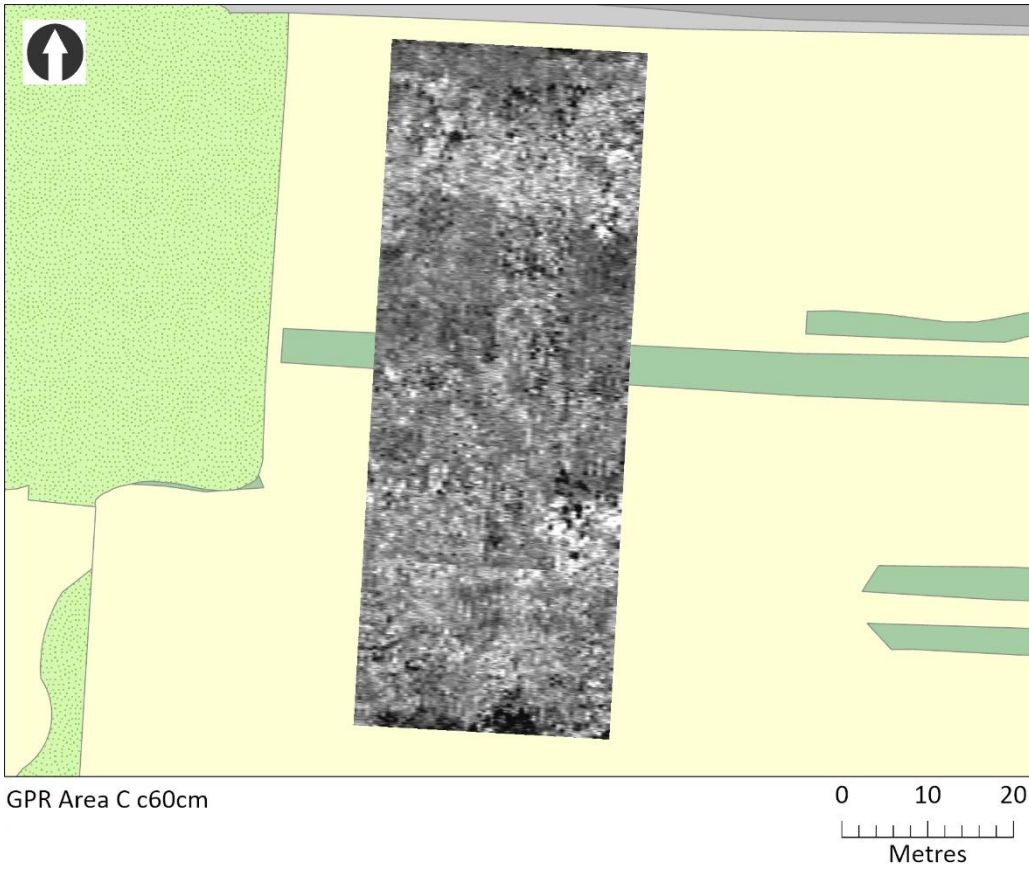


Figure 30 - Plot of GPR data at c60cm depth

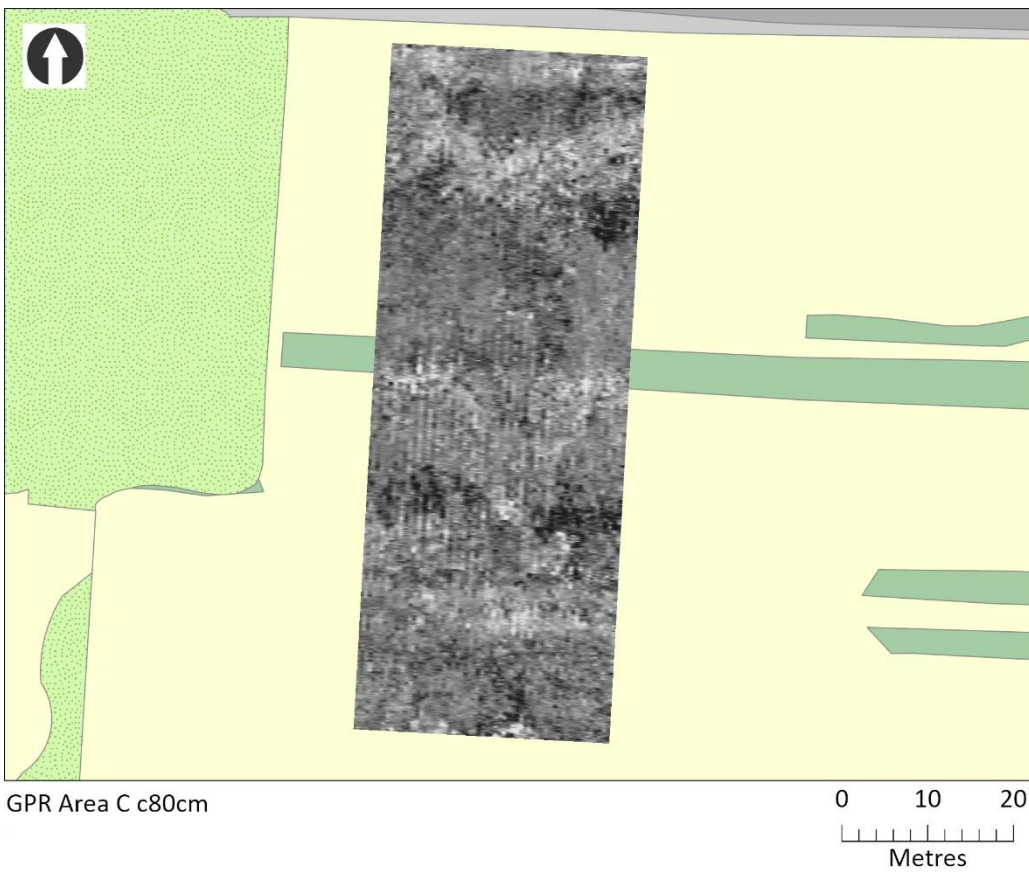


Figure 31 - Plot of GPR data at c80cm depth

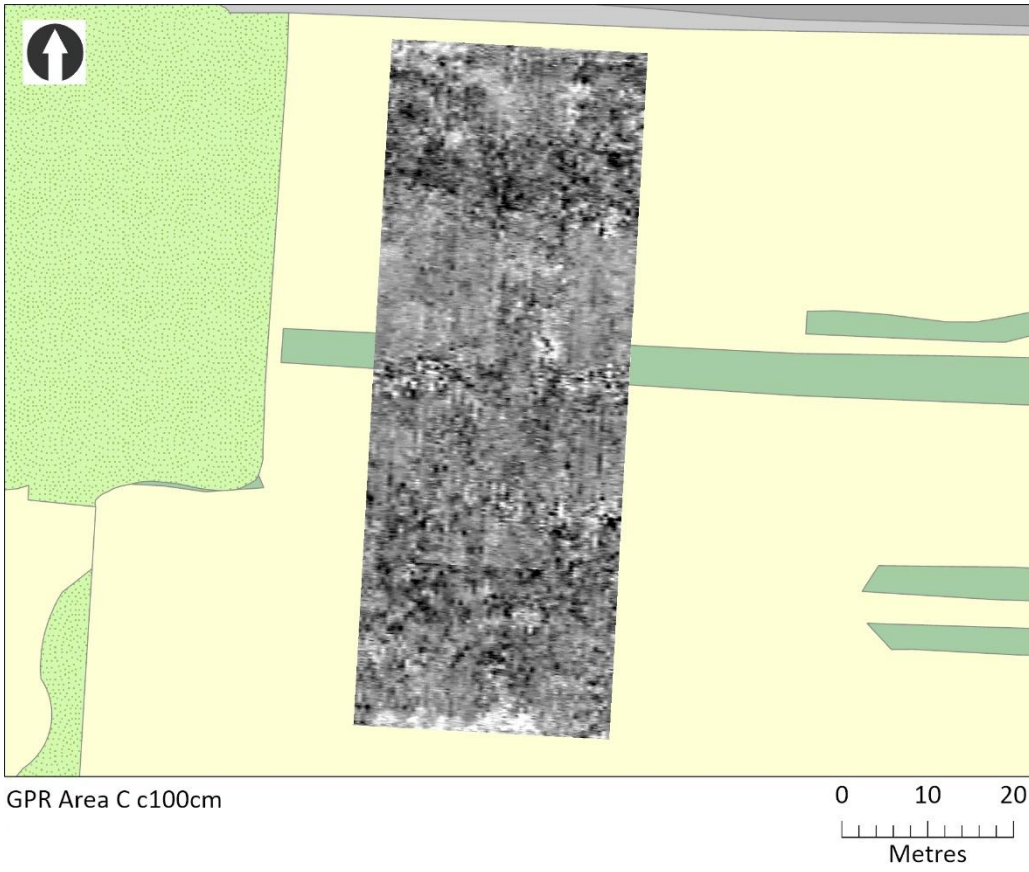


Figure 32 - Plot of GPR data at c100cm depth

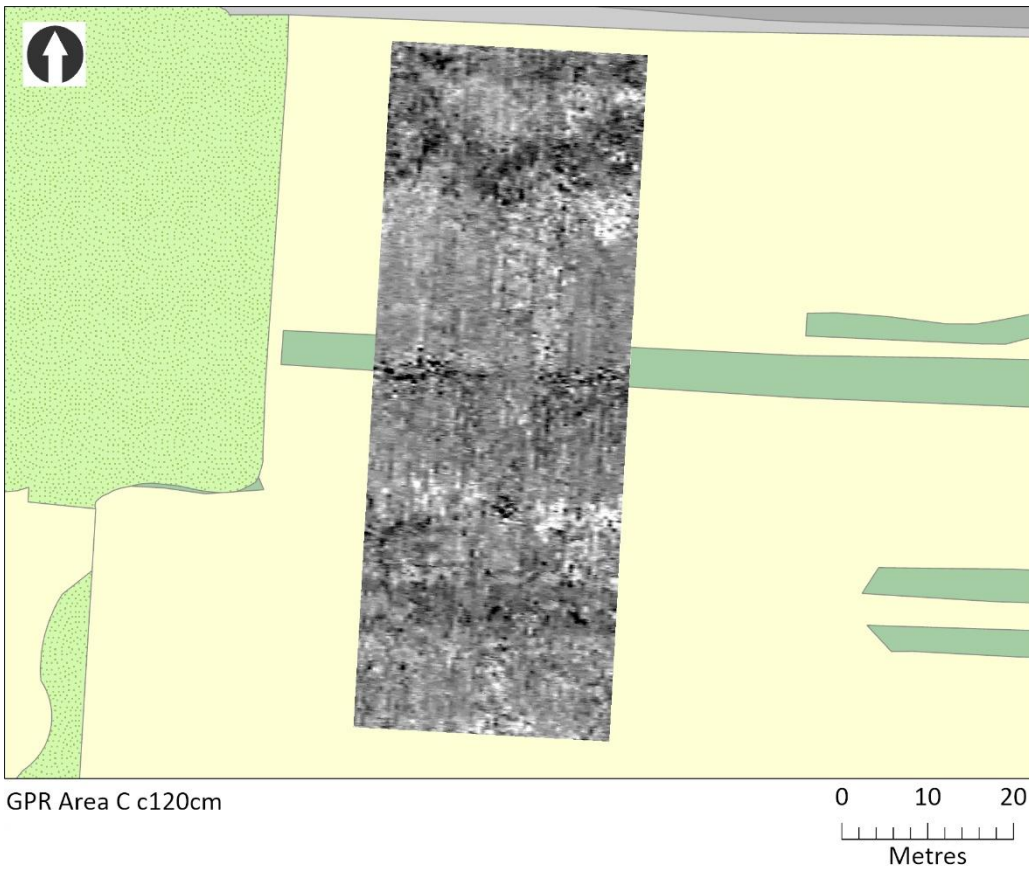


Figure 33 - Plot of GPR data at c120cm depth



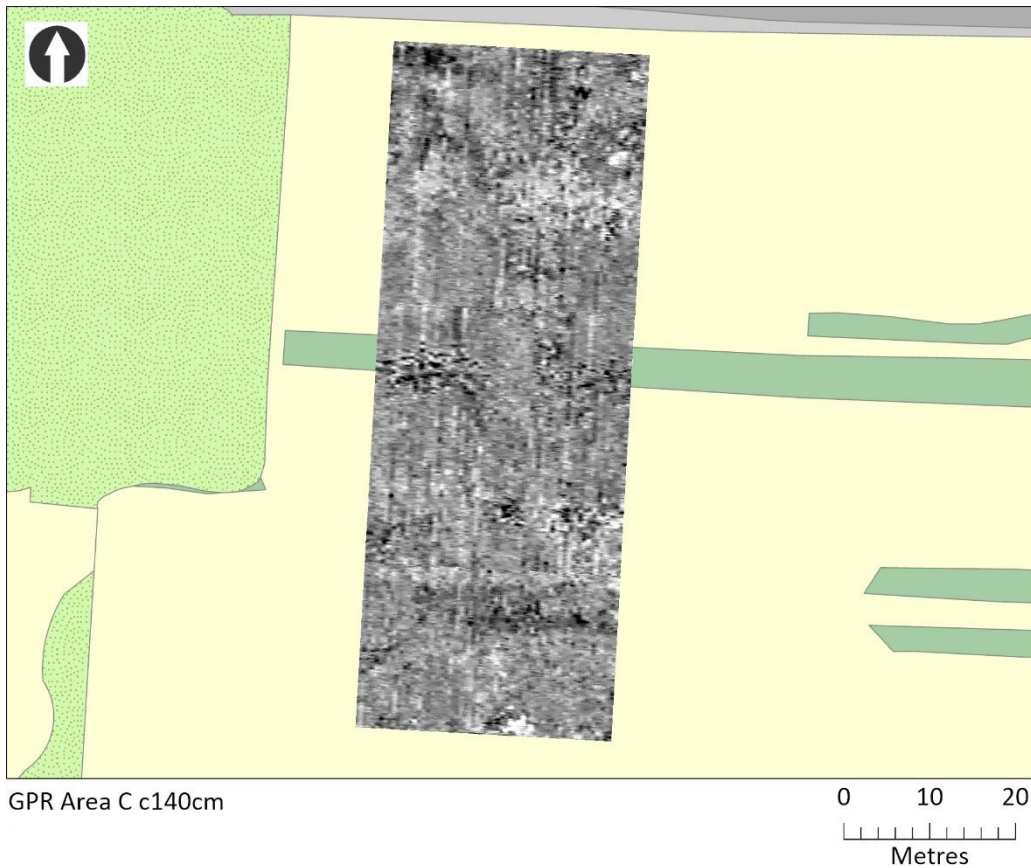


Figure 34 - Plot of GPR data at c140cm depth

### Processing flow

The data was imported in ReflexW 9.5.6 and processed using the DEWOW filter with the aim of removing possible lower frequency parts of the signal. Correction of the position of first arrival within each profile was undertaken using the Static Correction tool and a Manual Y Gain was applied to compensate for signal decay as the level of response diminished with increasing depth. A final Time Cut was applied to remove data below the maximum useable depth of each profile. The settings were applied as a batch process to all transects within the survey. The individual profiles were then combined, using the 3D module of ReflexW, to create a 3D surface generated from 2D lines. This enabled the generation of XY slices to assist interpretation. This sequence was captured as .MPEG video file and subsequently sampled to produce a series of bitmap images for presentation (Figures 28-34). Each of these slices represented a data sample at approximately 20cm depth intervals. Small errors in profile length and sample interval were corrected using the Trace Interpolation tool. This meant that all 2D profiles were combined within the 3D file with exactly the same number of traces and samples.

## **GPR - Interpretation**

### *Depth c.20cm*

[90]-[91] – These two linear responses, one negative and one positive, represent either side of the southern edge of the vallum.

[92]-[93] – These two weak negative linear responses coincide with the probable headland at the north edge of the field.

### *Depth c.40cm*

[87] – A positive response representing one side of the southern edge of the vallum. This is only visible on the eastern side of the survey area.

[88]-[89] – Two negative responses that represent either side of the northern edge of the vallum. There is a break in response between these two features.

[86] – This is equivalent to the response seen at [92] in the 20cm plot.

### *Depth c.60cm*

[84]-[85] – Two weak positive linear responses that represent either side of the southern edge of the vallum.

### *Depth c.80cm*

[79]-[80] – These strong positive and negative bands represent either side of the southern edge of the vallum.

[81]-[82] – Two weak negative responses that represent either side of the northern edge of the vallum.

[83] – A weak positive band at the northern edge of the field. They may represent the makeup of a former headland.

### *Depth c.100cm*

[77]-[78] – Two very weak negative linear features representing either side of the southern edge of the vallum.

[75]-[76] - Two very weak negative linear features representing either side of the northern edge of the vallum.

### *Depth c.120cm*

[70]-[71] - These strong positive and negative bands represent either side of the southern edge of the vallum.

[72]-[73] - Two weak negative responses that represent either side of the northern edge of the vallum. There is a break in response between these two features.

[74] - A negative band at the northern edge of the field. This may represent the makeup of a former headland.

### *Depth c.140cm*

[64]-[65] – These strong positive and negative bands represent either side of the southern edge of the vallum. There is no response for [65] at the western edge of the survey area.

[66]-[67] – Two weak negative responses that represent either side of the northern edge of the vallum. There is a break in response between these two features.

[68]-[69] – Two weak negative linear responses that do not correspond to any known features.

**GPR – Interpretation overlays**

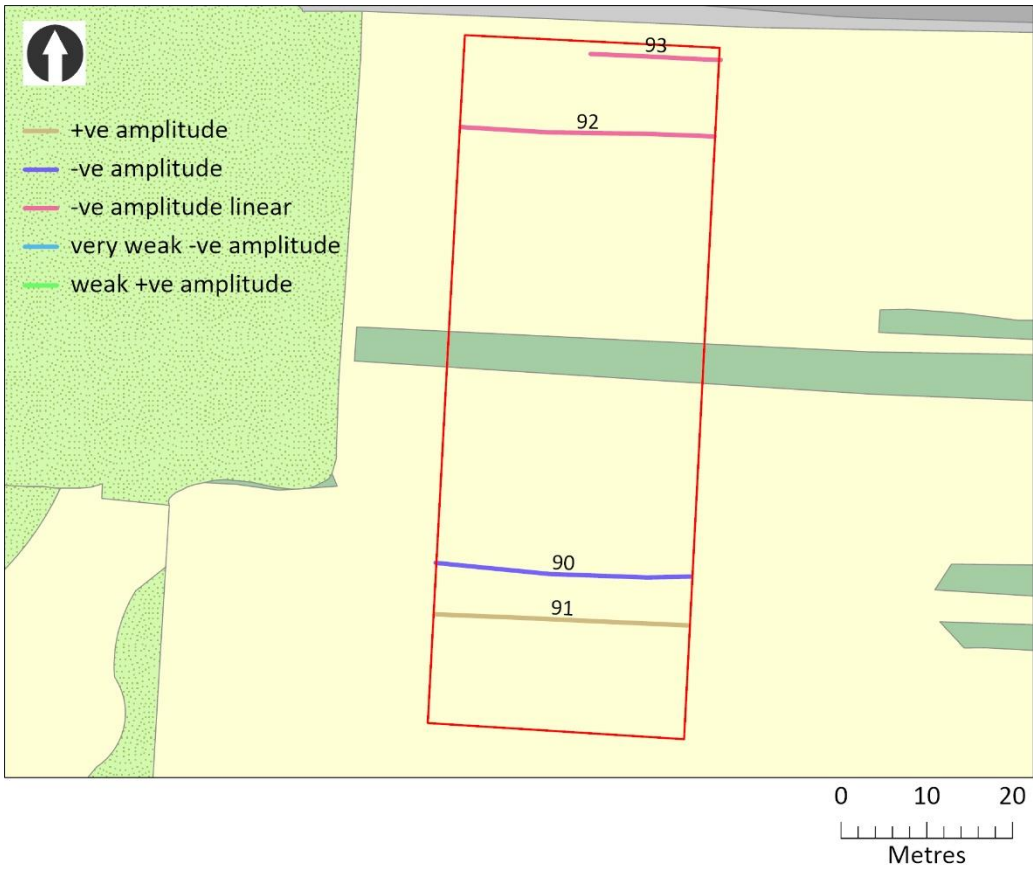


Figure 35 - Interpretation of the GPR survey at c20cm depth

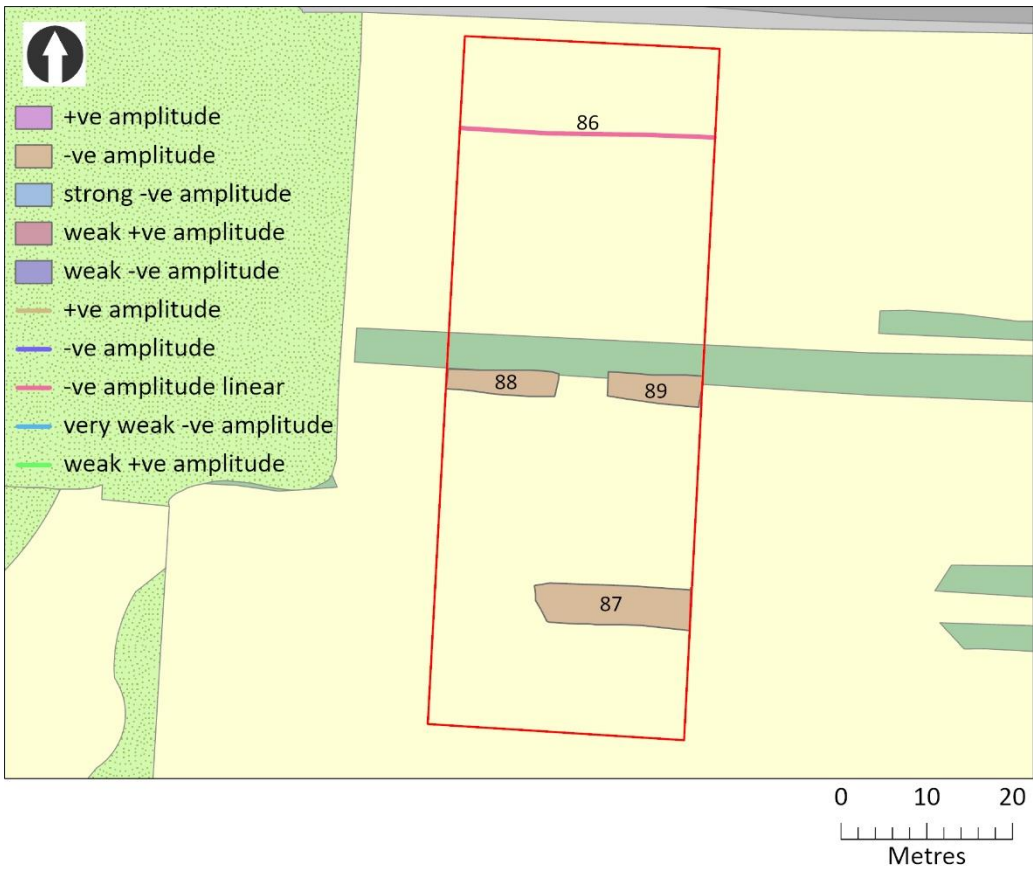


Figure 36 - Interpretation of the GPR survey at c40cm depth



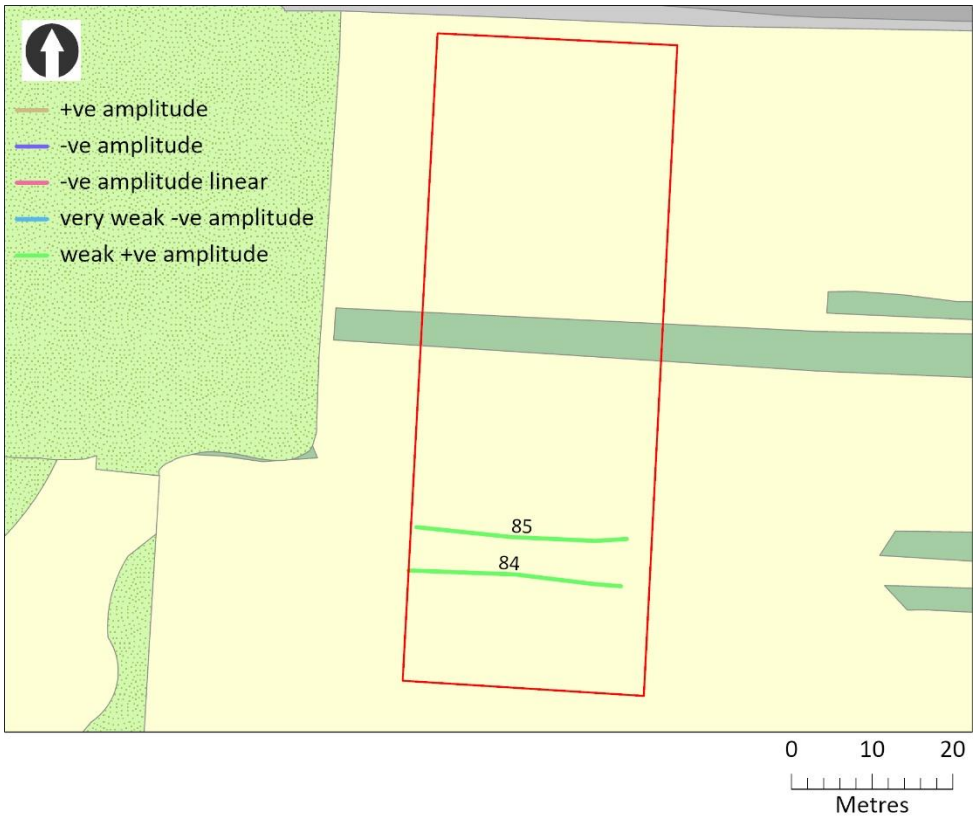


Figure 37 - Interpretation of the GPR survey at c60cm depth

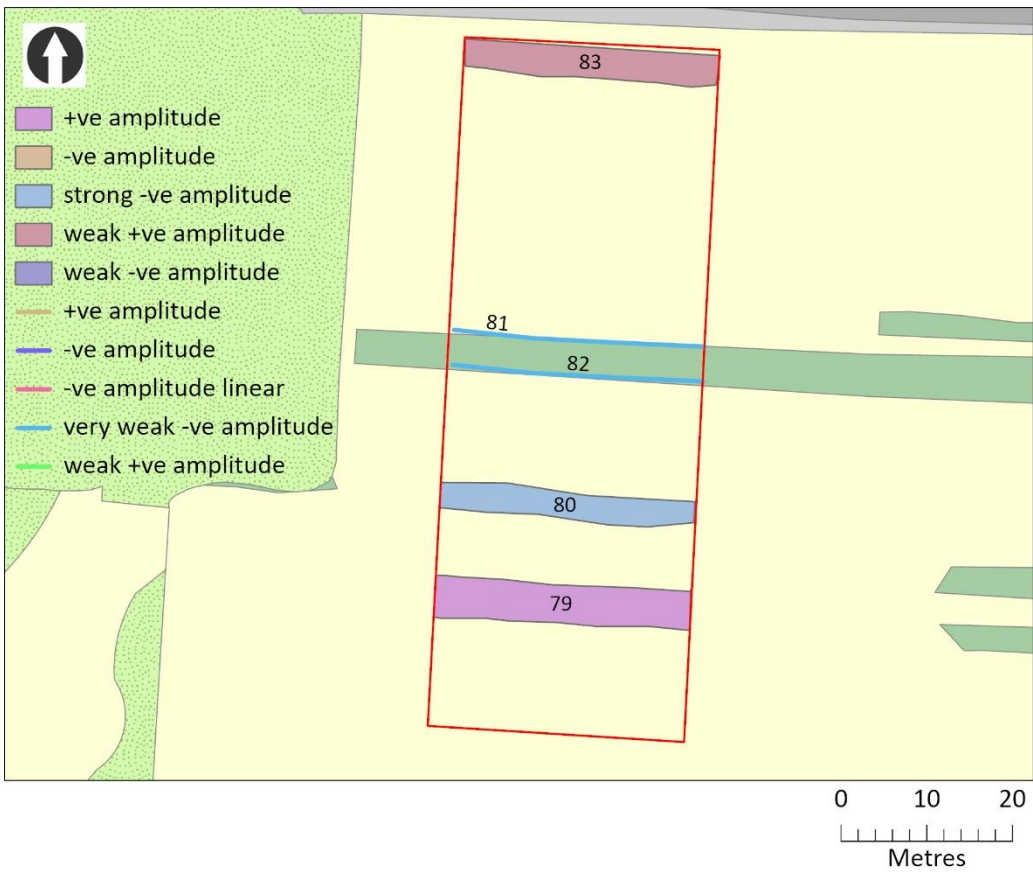


Figure 38 - Interpretation of the GPR survey at c80cm depth

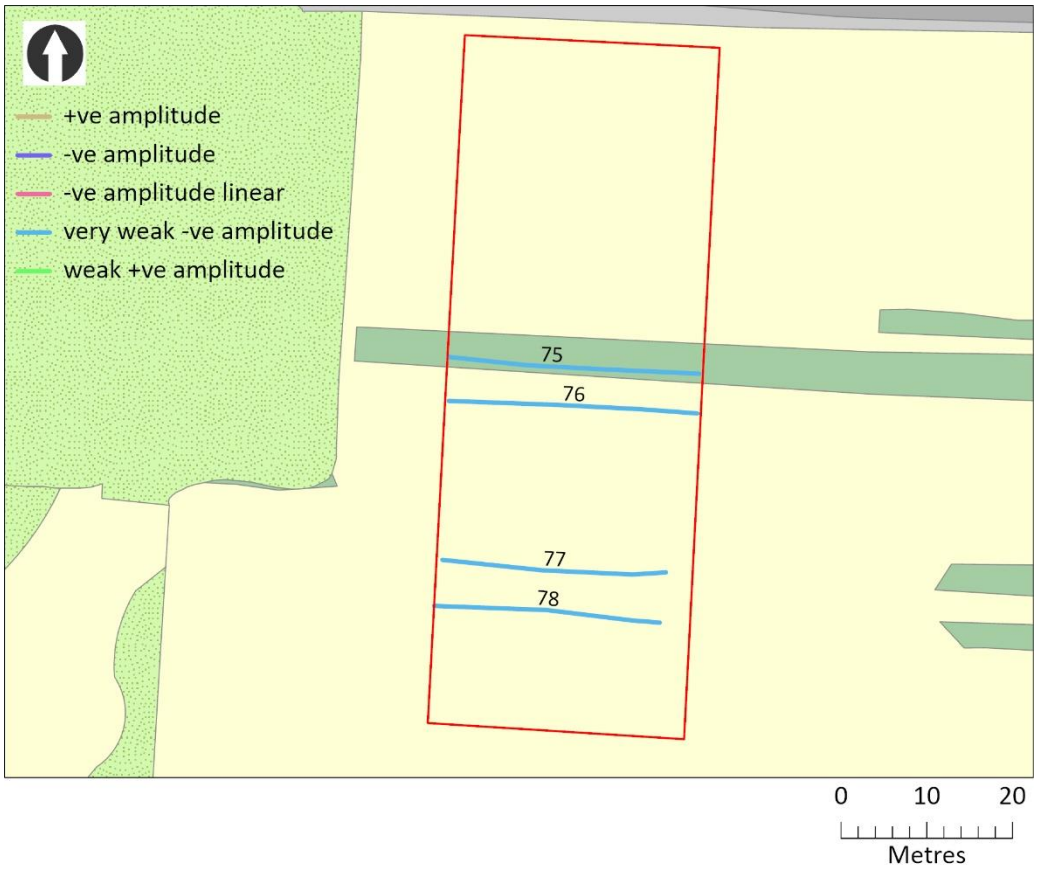


Figure 39 - Interpretation of the GPR survey at c100cm depth

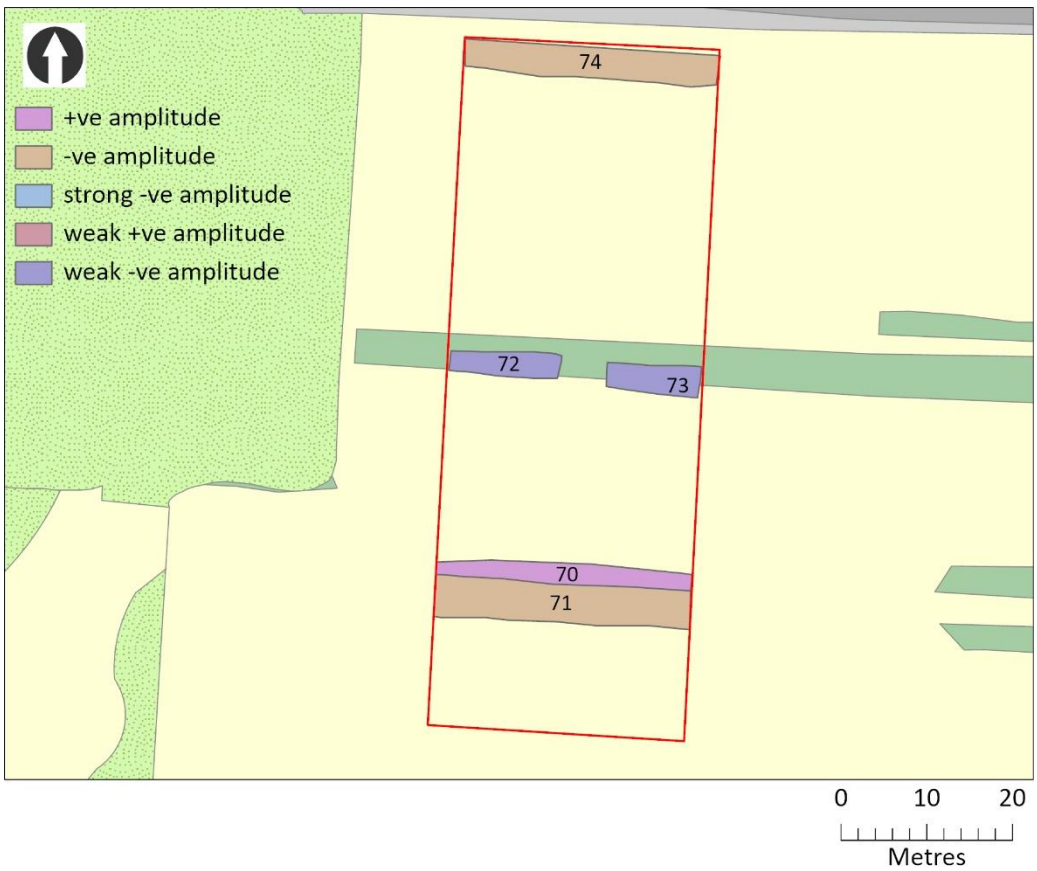


Figure 40 - Interpretation of the GPR survey at c120cm depth

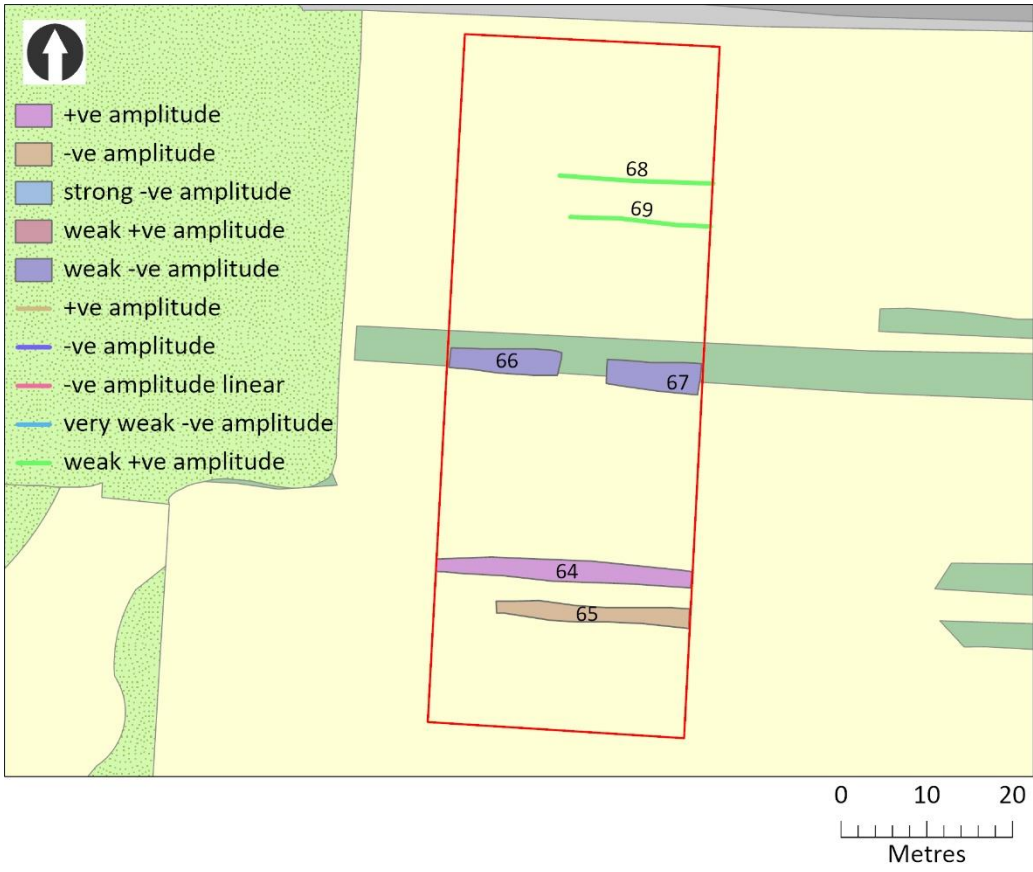


Figure 41 - Interpretation of the GPR survey at c140cm depth



## Gradiometer – plots of results

The data was processed using Geoplot 4 and exported as a raster image to the ArcGIS 7.1 project for the survey (Figures 11 and 12). Only basic processing was necessary within Geoplot 4. The grids were despiked with a threshold of  $\pm 3SD$  and the Zero Mean Traverse filter was applied to reduce any striping as a result of changes in the orientation of the gradiometer during zig-zag survey. A uniform High Pass Filter, to filter any changes in the geological background, was applied with a window of 10 readings in both the X and Y direction. Interpolation was carried out between traverses so that the final data had an X and Y resolution of 0.25 metres. The plots were then scaled and georeferenced to the British National Grid in ArcGIS using coordinates derived from the differential GNSS.

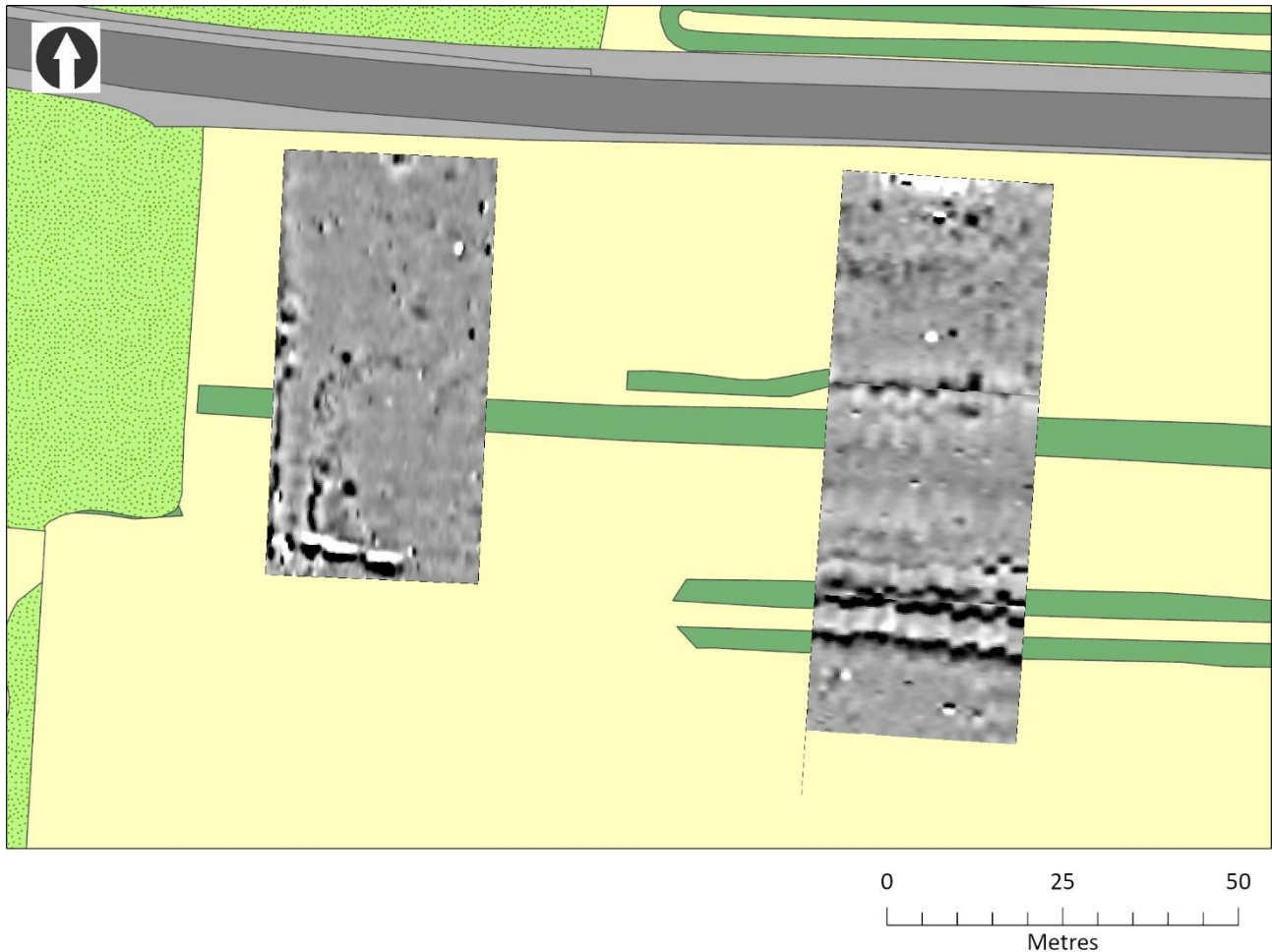


Figure 42 - Plot of gradiometer survey results - Areas A and B 2018

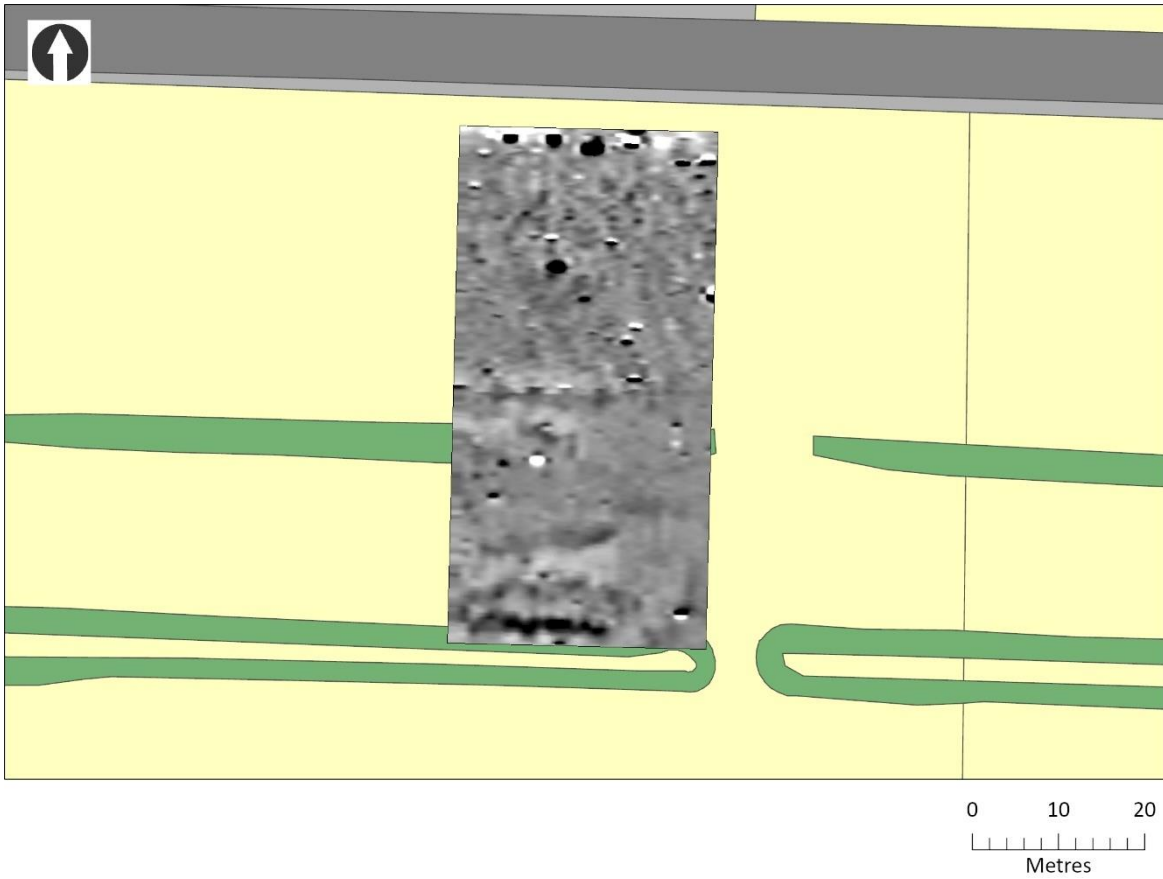


Figure 43 - Plot of gradiometer survey results - Area C 2018

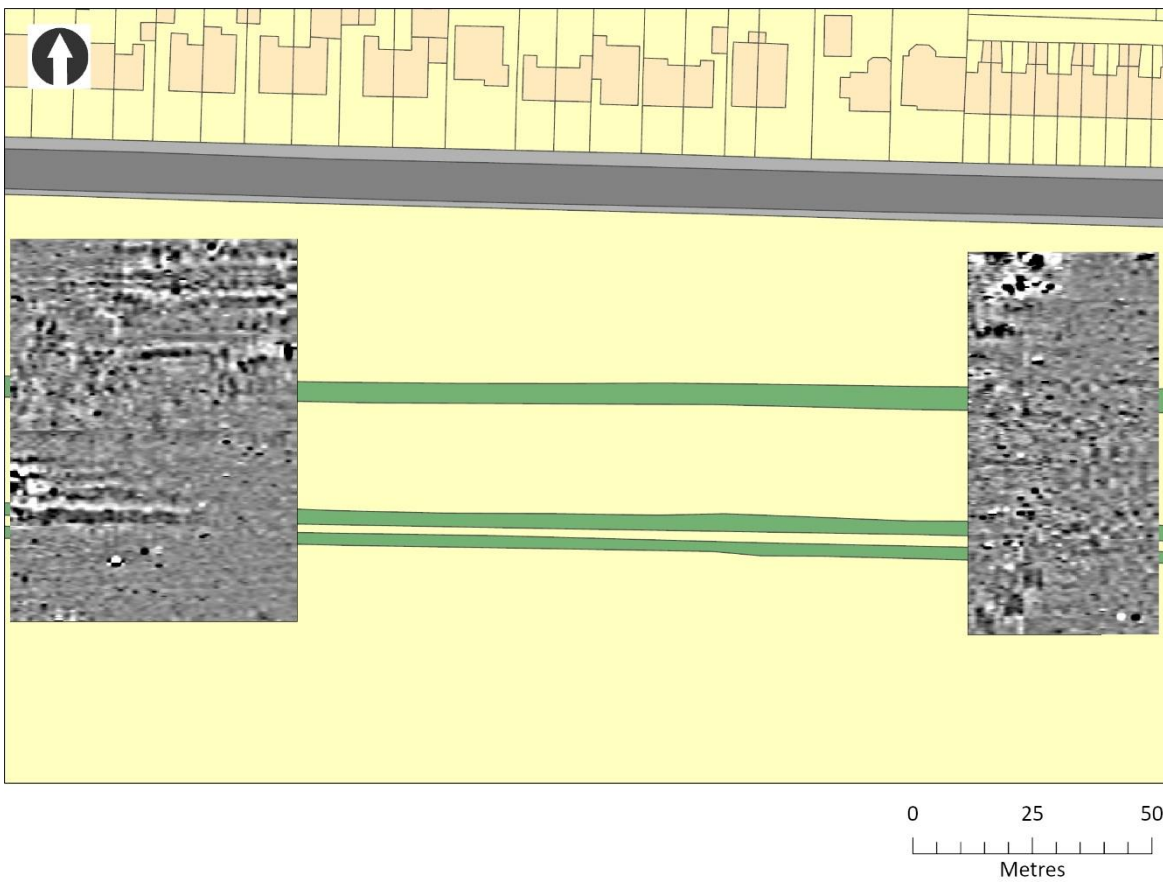


Figure 44 - Plot of gradiometer survey results - Areas 1 and 2 2019

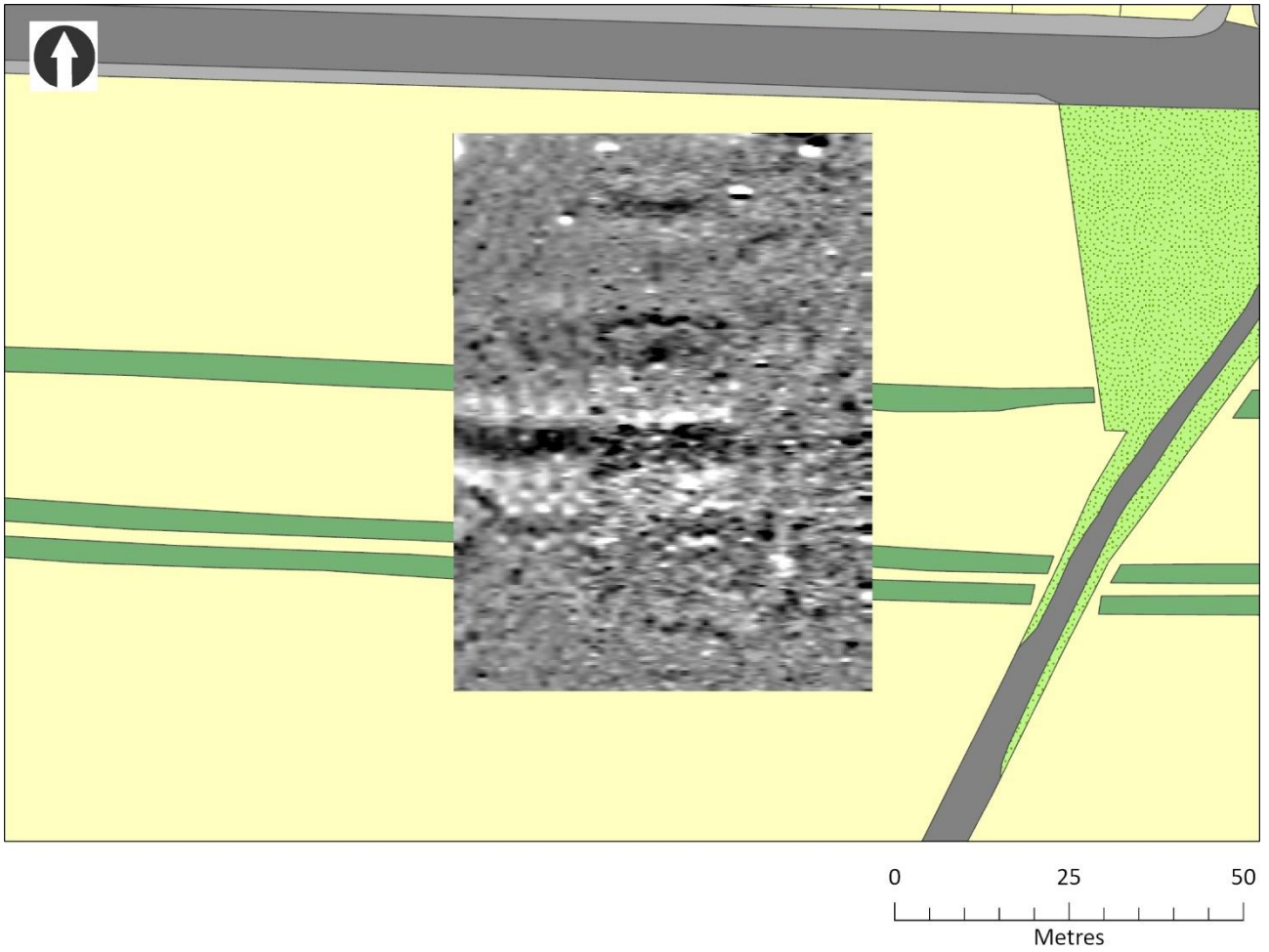


Figure 45 - Plot of gradiometer survey results - Area 3 2019



## Gradiometer Overlays

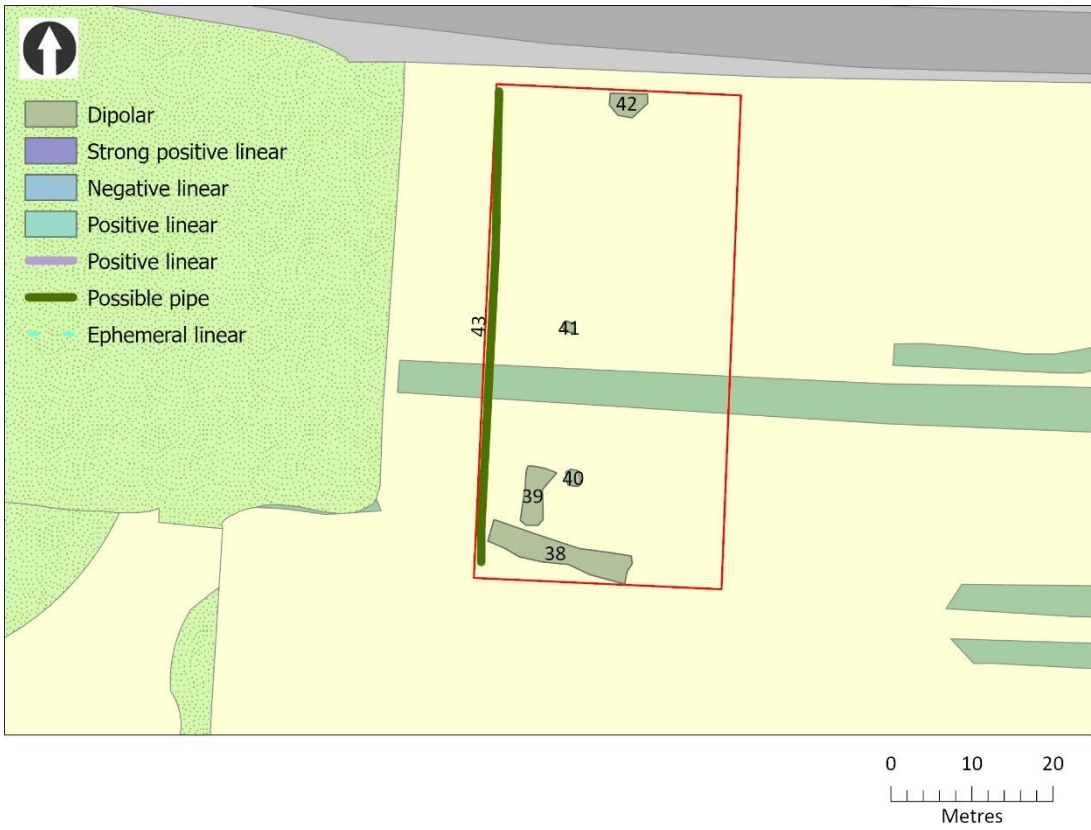


Figure 46 - Interpretation of gradiometer survey results - Area A 2018

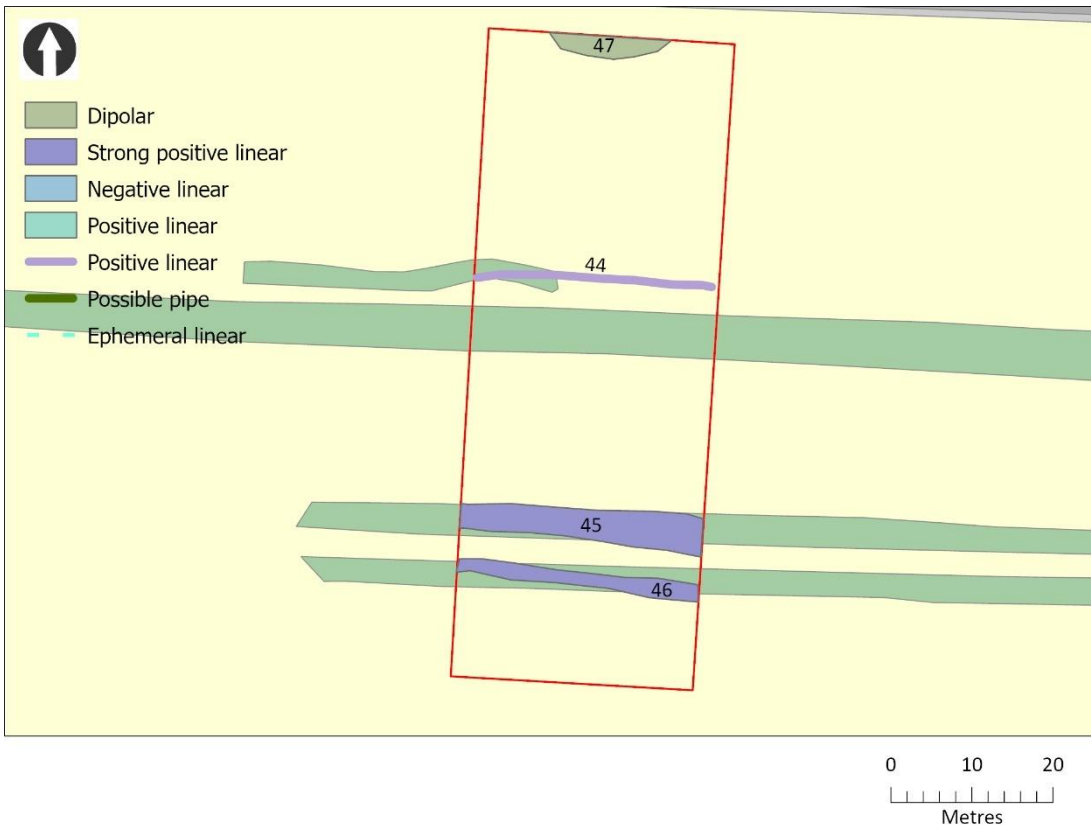


Figure 47 - Interpretation of gradiometer survey results - Area B 2018

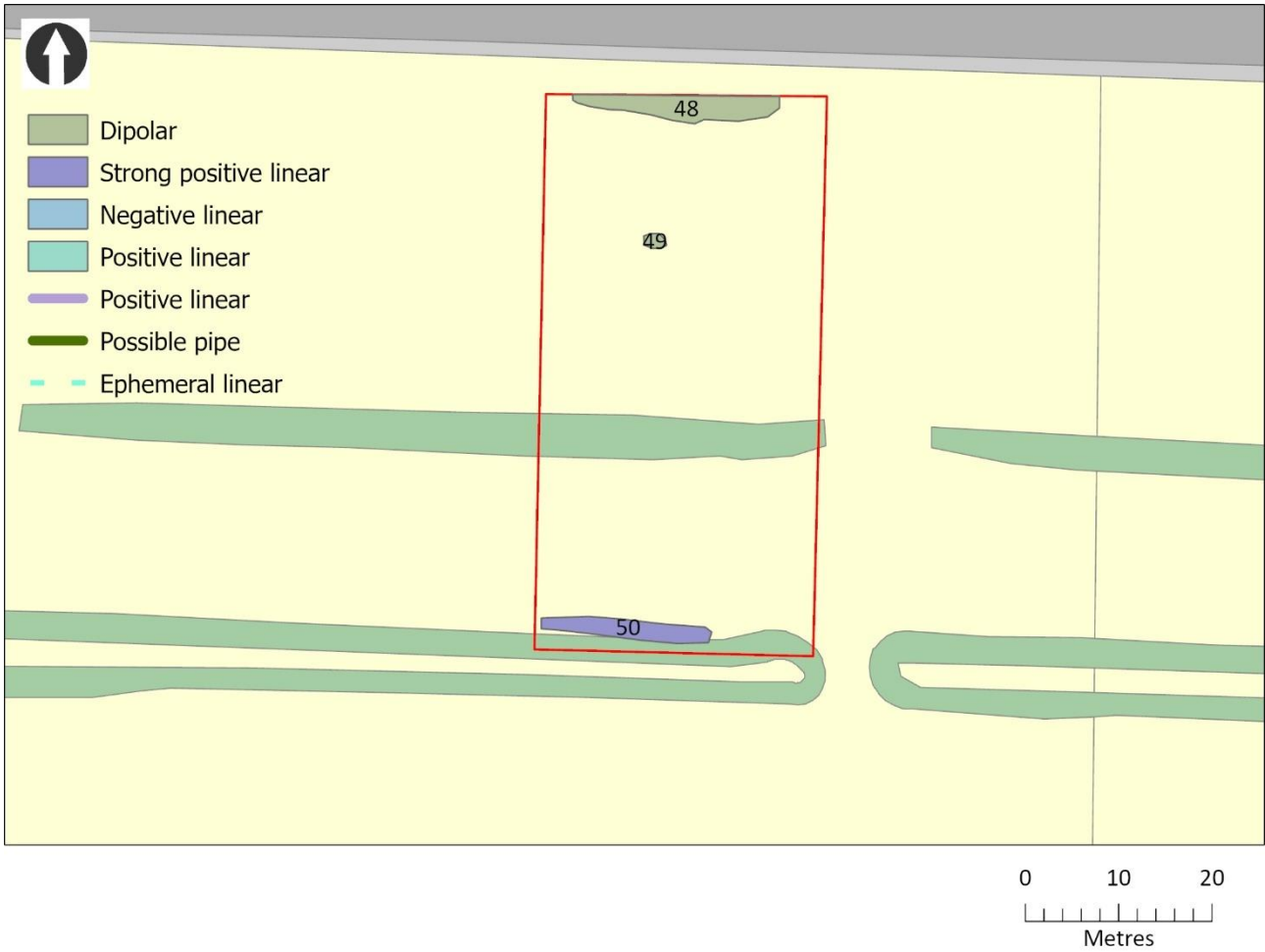


Figure 48 - Interpretation of gradiometer survey results - Area c 2018

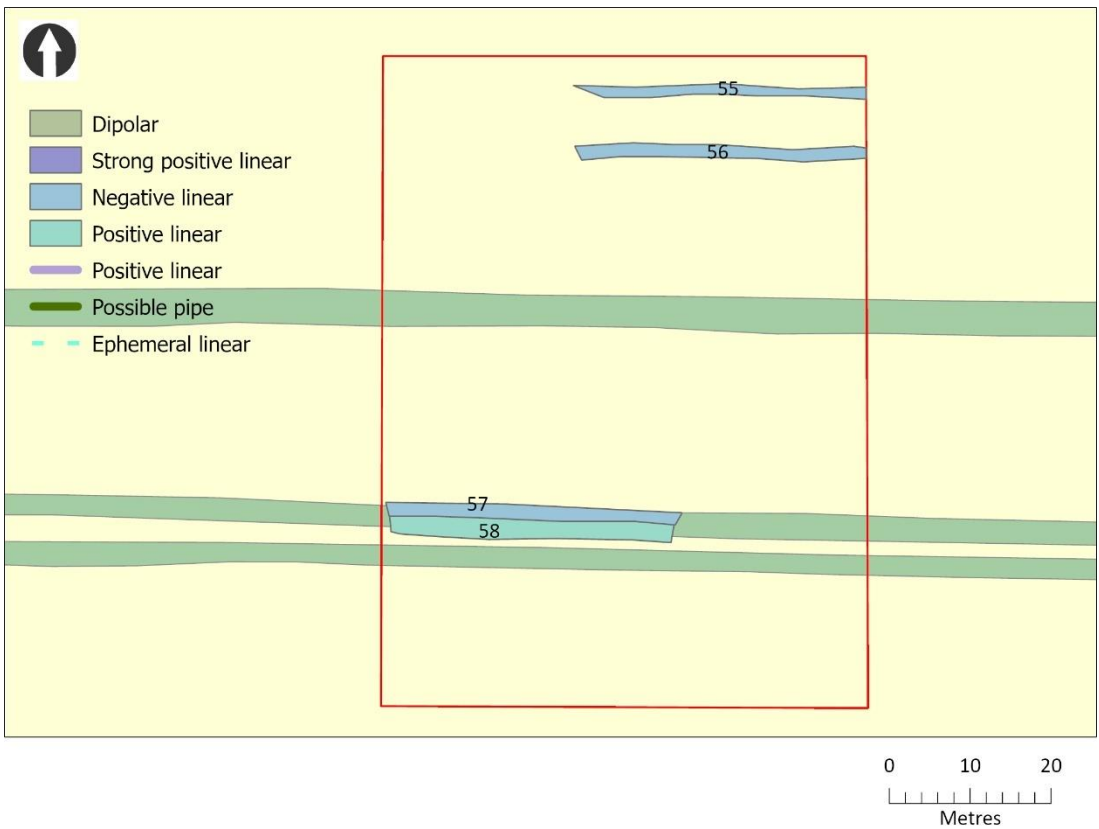


Figure 49 - Interpretation of gradiometer survey results - Area 1 2019

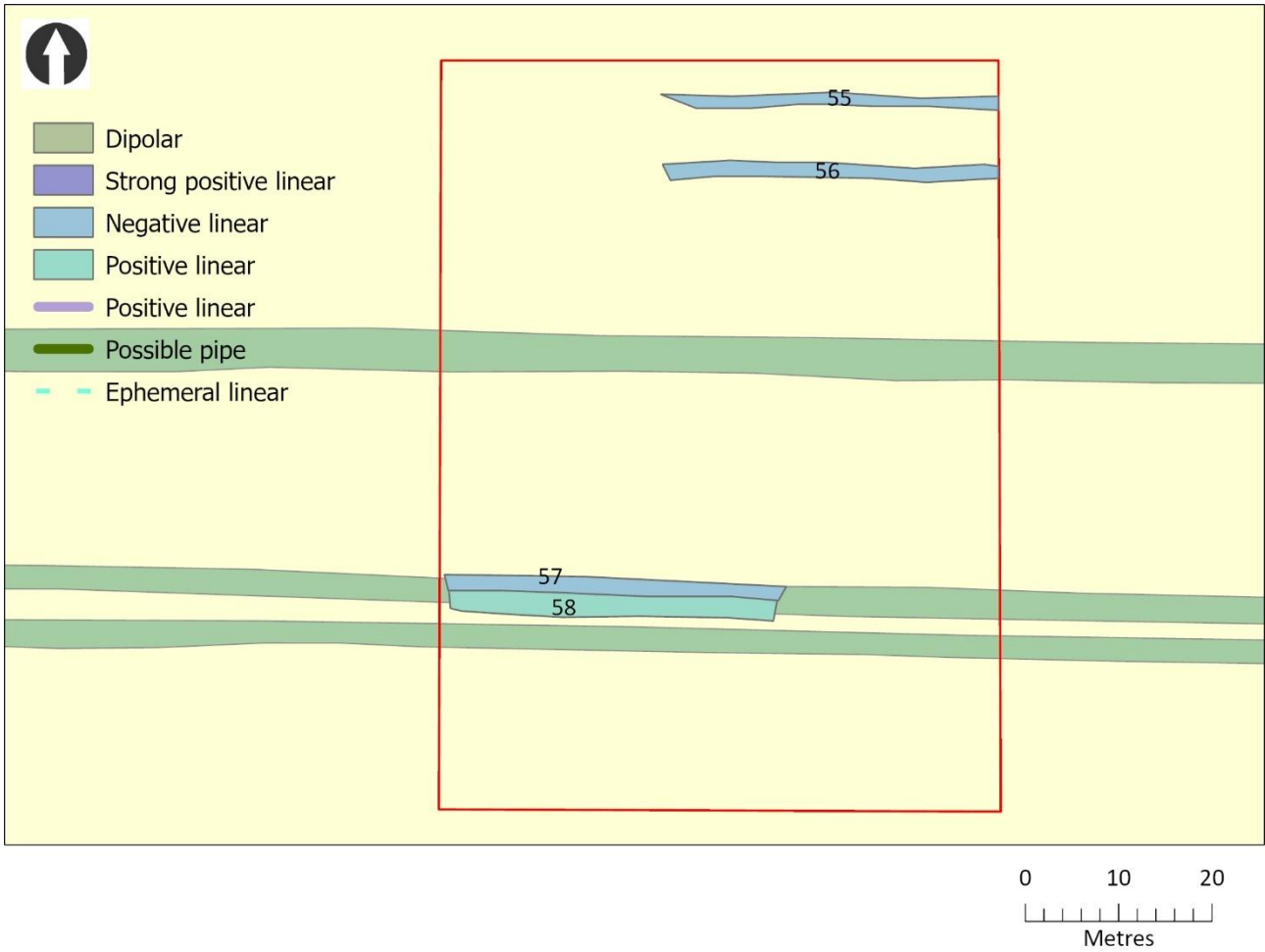


Figure 50 - Interpretation of gradiometer survey results - Area 2 2019

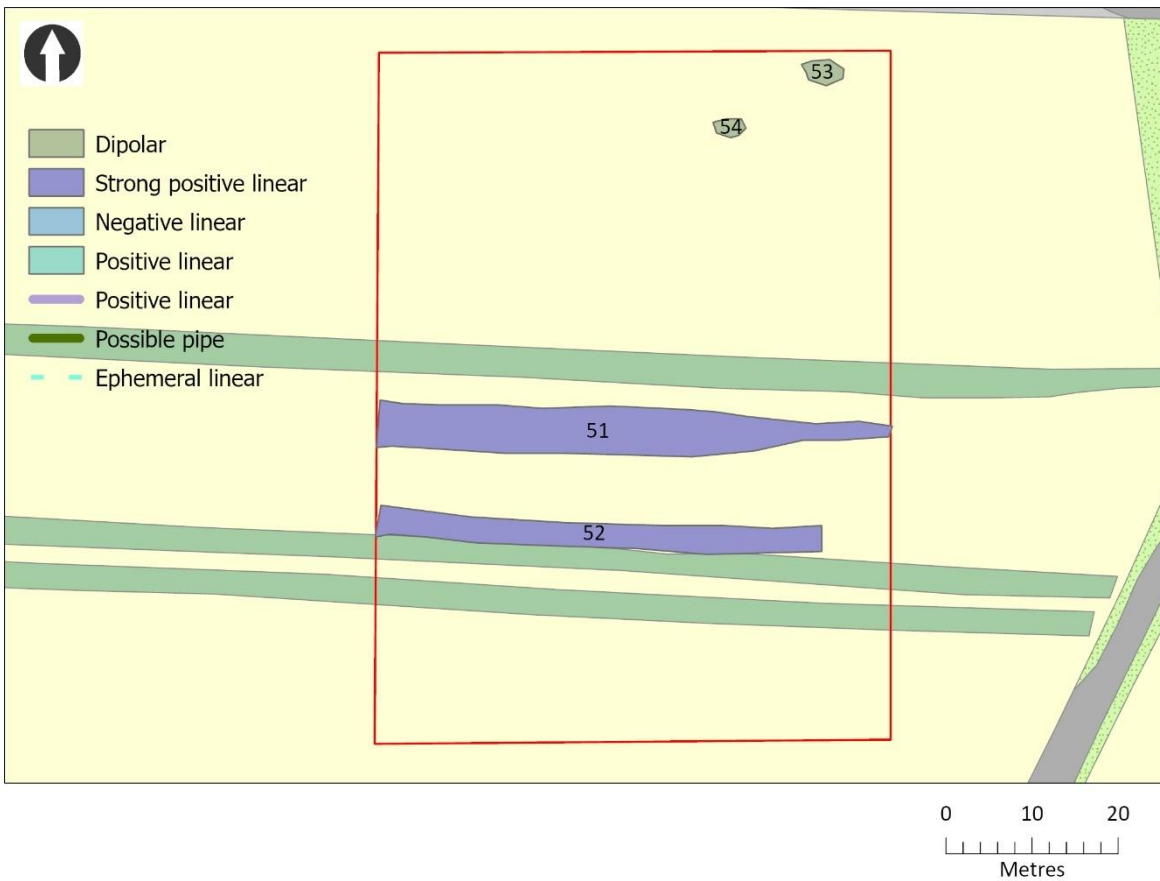


Figure 51 - Interpretation of gradiometer survey results - Area 3 2019



## **Gradiometer – Interpretation**

### *Area A 2018*

[43] – A strong positive linear response on the western edge of the survey area. This could be a pipe or field drain that shows as disturbance at the edge of the vallum.

[38] – A strong dipolar response that may represent ferrous material dumped in the southern edge of the vallum. The response only covers part of the width of the survey area.

[39]-[42] Dipolar responses from buried ferrous litter.

### *Area B 2018*

[45]-[46] – Strong positive linear responses that represent the southern edge of the vallum.

[44] – A strong linear response from the north edge of the vallum.

[47] – A dipolar response at the edge of the field caused by a combination of metal wire and probable buried ferrous litter.

### *Area C 2018*

[50] – A partial strong linear positive response representing the southern edge of the vallum. The gap in the response on the eastern side of the survey area does not correspond to that on the map.

### *Area 1 2019*

[62]-[63] – Ephemeral positive linear feature that represents the northern edge of the vallum.

[60]-[61] - Ephemeral positive linear feature that represents the southern edge of the vallum.

[59] – Large dipolar response(s) that probably represents buried ferrous litter.

### *Area 2 2019*

[57]-[58] – A dipolar response at the southern edge of the vallum. This is only visible in part of the survey area.

[55]-[56] – Parallel linear negative responses at the northern end of the survey area that only cover part of the width of the area surveyed. It is unclear as to what these represent.

### *Area 3 2019*

[51]-[52] – Strong positive linear features that represent the inner northern and southern margins of the vallum.

[53]-[54] – Dipolar response to buried ferrous litter.

## **Resistivity Results – process summary**

The data was processed using the same software as the gradiometer survey. The data was despiked with a threshold of +/- 3SD and then a Gaussian high pass filter was applied with a window of 10 readings in the x and y directions to minimise the effect of background geology. A low pass filter with a window of 1 reading in both the X and Y directions was used to smooth the data and enhance any large weak features. Interpolation of the data was carried out in the X and Y directions to give data plots with a final spatial resolution of 0.25m x 0.25m. This was an equivalent resolution to the gradiometer data.

## Resistivity – plot of results

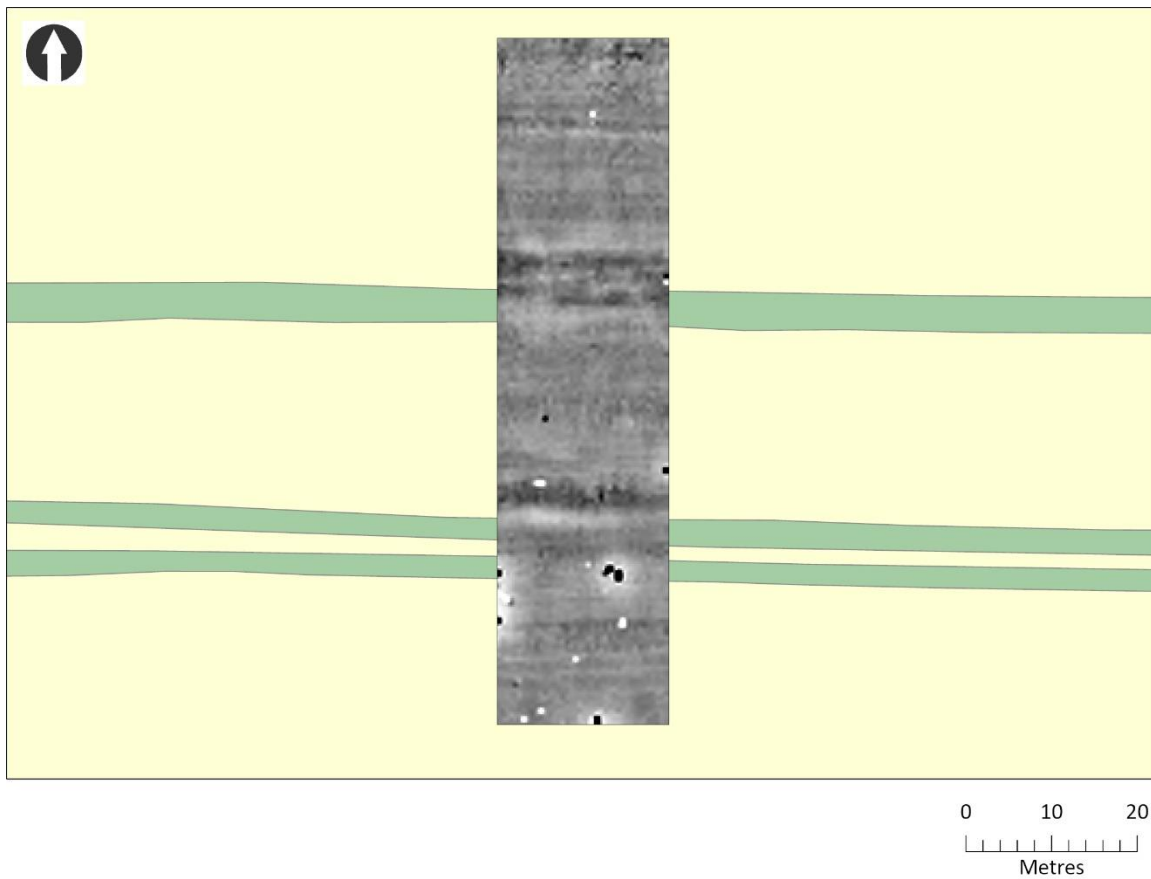


Figure 52 - Plot of the resistivity survey results - Area 2 September 2019

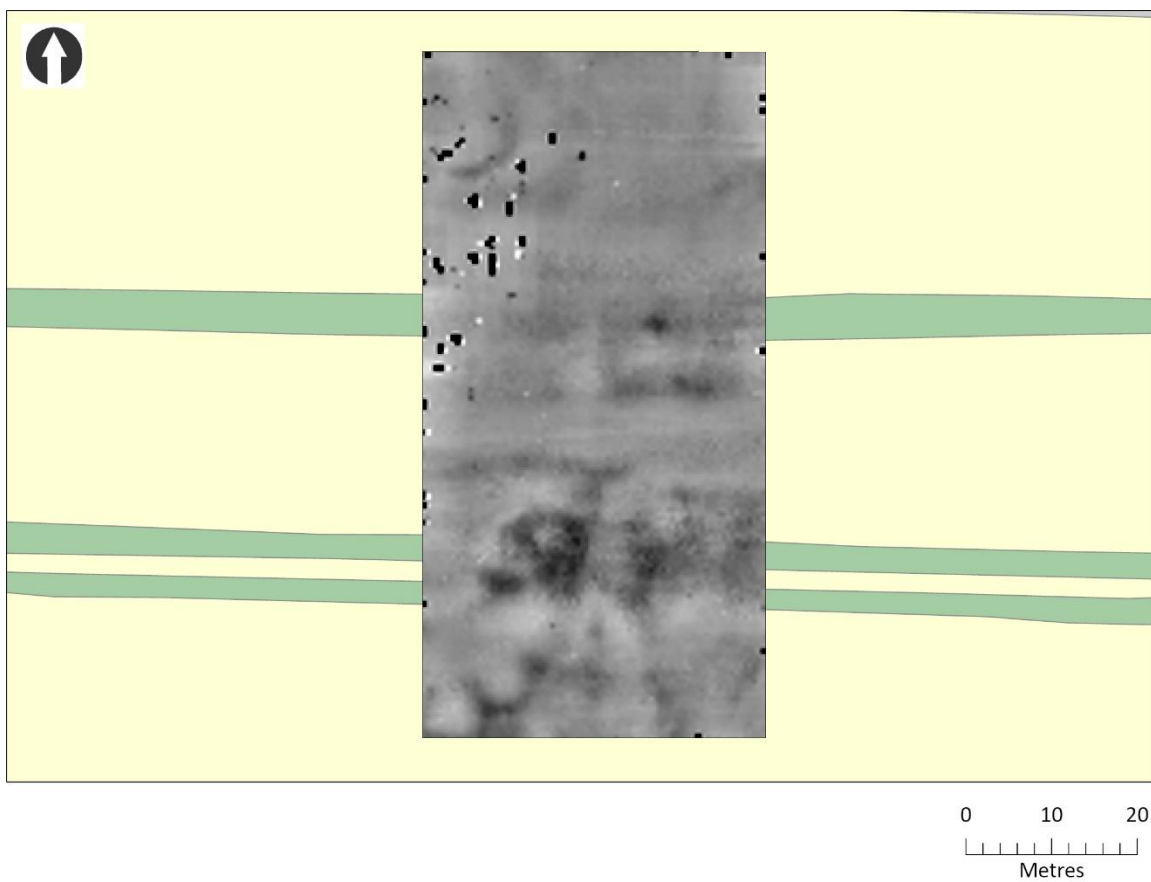


Figure 53 - Plot of the resistivity survey results - Area 1 September 2019

## Resistivity – Interpretation Overlays

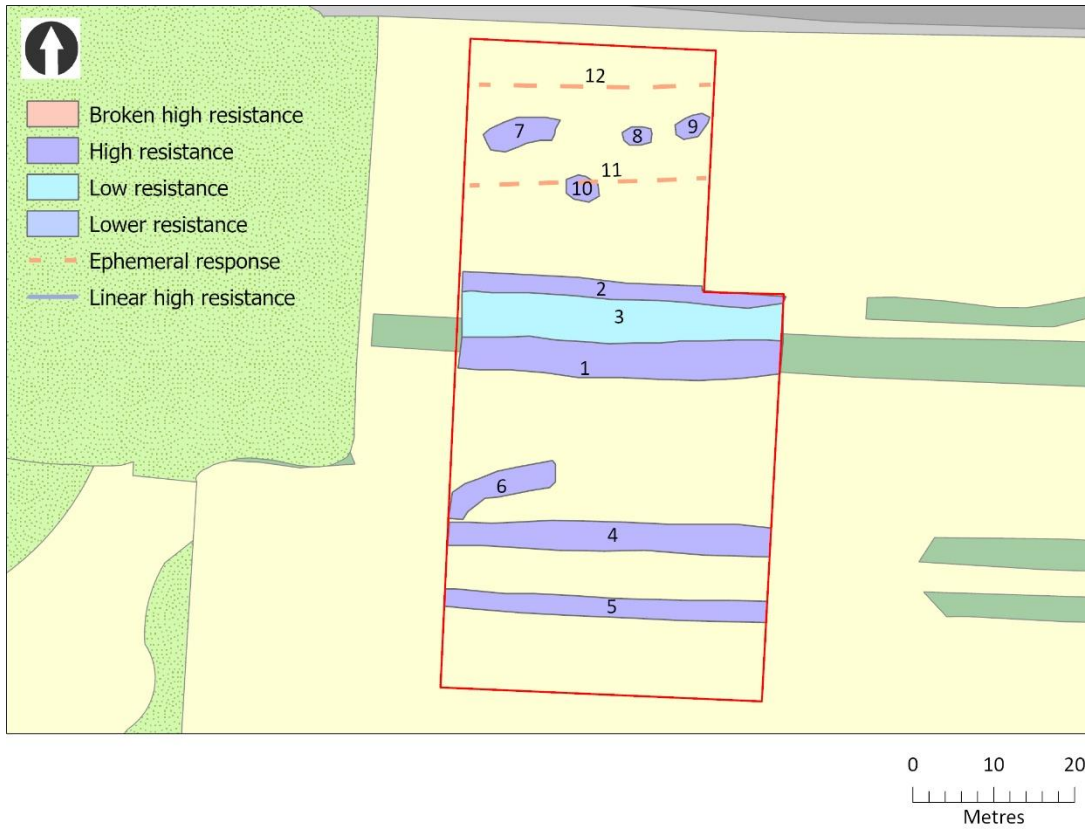


Figure 54 - Interpretation of the resistivity survey results - March 2019

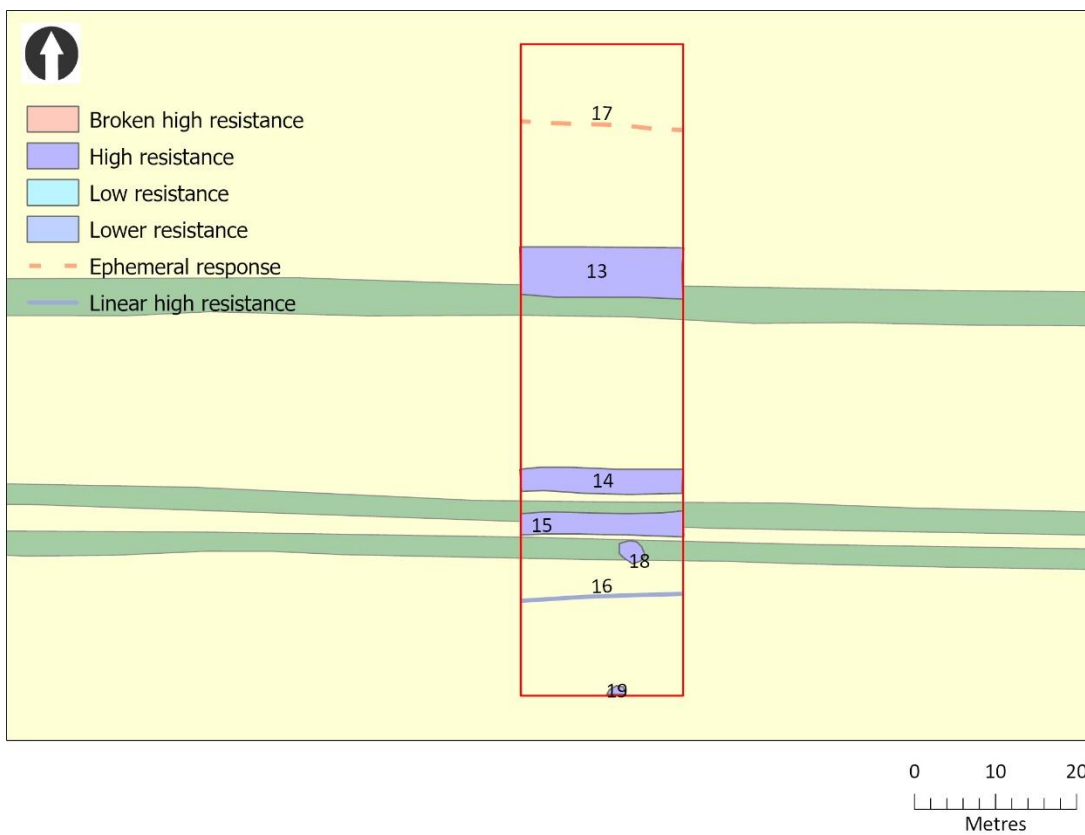


Figure 55 - Interpretation of the resistivity survey results - Area 2 September 2019



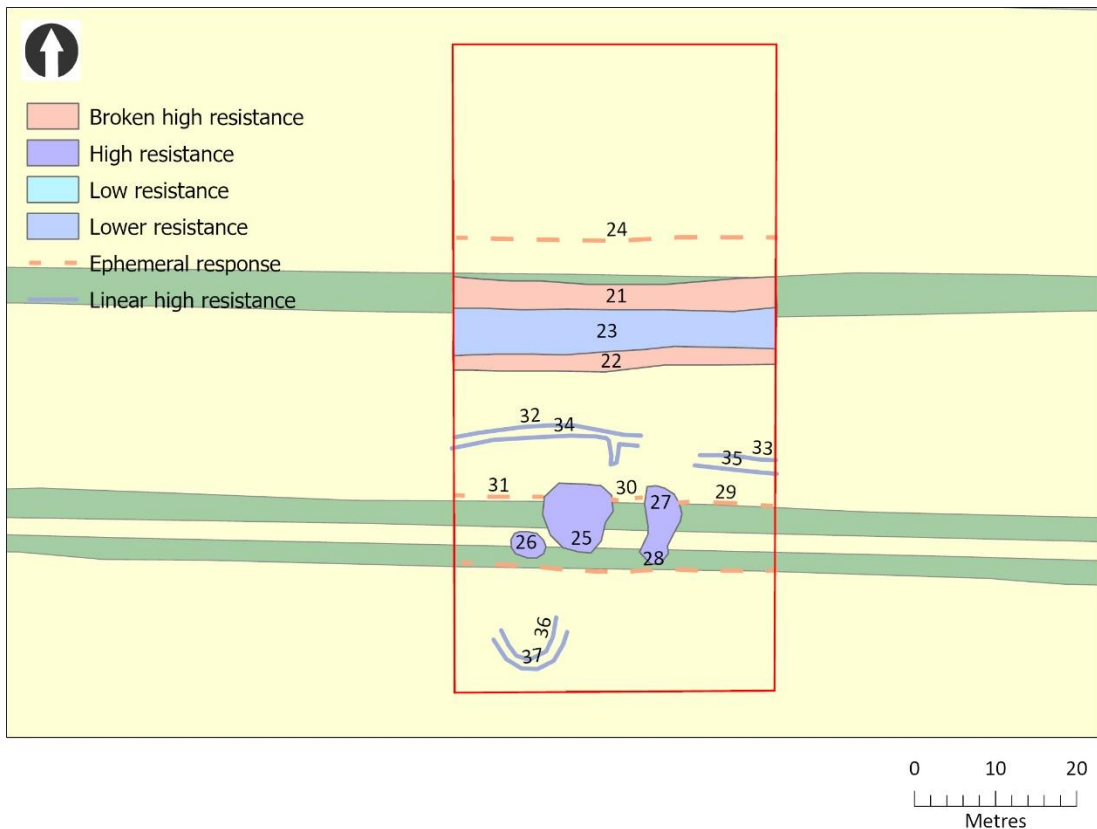


Figure 56 - Interpretation of the resistivity survey results - Area 1 September 2019

## Resistivity – Interpretation

### Area A March 2019

- [1]-[2] – High resistance linear features that flank an area of low resistance [3] and are the response from the northern edge of the vallum.
- [3] – A linear area of low resistance between [1]-[2]. This may be reflective of the mixture makeup of the vallum.
- [4]-[5] – Two linear bands of high resistance that demark the southern edge of the vallum.
- [6] – A curvilinear band of high resistance that may represent a dump of material within the vallum.
- [7]-[10] – Patches of high resistance that have no obvious pattern and may be variations in the buried geology.
- [11]-[12] – Two very ephemeral east-west linear responses. It is unclear as to what these represent.

### Area 2 September 2019

- [14]-[15] – Two linear bands of high resistance that demark the southern edge of the vallum.
- [13] – A linear band of high resistance that demarks the northern edge of the vallum.
- [16]-[19] – Dipolar response from buried ferrous litter.
- [17] – Weak ephemeral linear response of unknown significance.
- [16] – A Line of high resistance of unknown significance.

### Area 1 September 2019

- [21]-[22] - High resistance linear features that flank an area of low resistance [23] and are the response from the northern edge of the vallum.

[23] - A linear area of low resistance between [21]-[22]. This may be reflective of the mixed makeup of the vallum.

[24] – A weak ephemeral linear response of unknown significance.

[25]-[27] – Ferrous litter in the southern edge of the vallum.

[28]-[31] - Two very ephemeral east-west linear responses. It is unclear as to what these represent.

[32]-[35] – Curvilinear lower resistance feature at the centre of the line of the vallum. These probably represent increased moisture levels along the line of the base of the vallum.

[36]-[37] – Two high resistance curvilinear features south of the line of the vallum. This might be the result of early coal workings.

Area 1 had a large number of dummy readings in its northwest corner. This was largely due to its proximity to the field entrance and was presumably the result of the addition of extra metal in this area.

## Summary

There was reasonable success with all the geophysical methods employed with the gradiometer survey probably the least successful at the of detection of sub-surface features. This is most likely due to the lack of magnetic material within the fill of the vallum itself. The resistivity survey was the most successful in detecting sub-surface features and clearly demonstrated the change in response across the area. The observed loss of the vallum on the surface at the eastern end, presumably due to ploughing, is mirrored in the sub-surface results from the resistivity. The GPR survey was relatively successful and the only technique to provide depth information for buried deposits. However, as with many other parts of the UK, the attenuation of signal due to high moisture levels and the resultant lack of depth penetration remains an issue.

## Sources and References

British Geological Survey (2011) - *Soil Parent Material Model [SHAPE geospatial data]*, Scale 1:50000, updated: 1 June 2011, BGS, using: EDINA Geology Digimap Service, <<https://digimap.edina.ac.uk>>, Downloaded: 2021-05-13 09:35:02.7

British Geological Survey (2016) *DiGMapGB-50 [SHAPE geospatial data]*, Scale 1:50000, updated: 30 November 2016, BGS, using: EDINA Geology Digimap Service, <<https://digimap.edina.ac.uk>>, Downloaded: 2021-05-13 09:35:02.7

Environment Agency (2016) *Lidar Composite Digital Terrain Model England 1m resolution [ASC geospatial data]*. Scale 1:4000, Updated: 5 January 2016, Open Government Licence, using: EDINA LIDAR Digimap Service, <<https://digimap.edina.ac.uk>>, Downloaded: 2021-05-13 09:37:04.87

Ordnance Survey (2021) *1:50,000 Scale Colour Raster [TIFF geospatial data]*, Scale 1:50,000, updated: 14 May 2021, Ordnance Survey (GB), Using: EDINA Digimap Ordnance Survey Service, <<https://digimap.edina.ac.uk>>, Downloaded: 2021-11-01 09:37:39.084

Schmidt A, Linford P, Linford N, David A, Gaffney C, Sarris A and Fassbinder J (2016) *EAC Guidelines for the use of Geophysics in Archaeology*

Simpson F, Hodgson K and Richmond I (1934) New Turret-Sites on the Line of the Turf Wall and the Type of Stone Wall Later Associated with Them in *Transactions of the Cumberland and Westmorland Antiquarian and Archaeological Society Series 2 Volume 34*